Robotica (2010) volume 28, pp. 563–581. © Cambridge University Press 2009
doi:10.1017/S0263574709990257

Parametric-based dynamic synthesis of 3D-gait

Guy Bessonnet*, Jérôme Marot, Pascal Seguin and Philippe Sardain

Laboratoire de Mécanique des Solides, CNRS-UMR6610, Université de Poitiers, SP2MI, Bd. M. & P. Curie, BP 30179, 86962 Futuroscope Chasseneuil cedex, France

(Received in Final Form: June 5, 2009. First published online: July 7, 2009)

SUMMARY

This paper describes a dynamic synthesis method for generating optimal walking patterns of biped robots having a human-like locomotion system. The generating principle of gait is based on the minimisation of driving torques. A parametric optimisation technique is used to solve the underlying optimal control problem. Special attention is devoted to foot-ground interactions in order to ensure a steady dynamic balance of the biped. Transition states between step sub-phases are fully optimised together with step length and sub-phase lengths with respect to a given walking velocity. The data needed to generate purely cyclic steps can be reduced to the forward velocity.

KEYWORDS: 3D-gait; Gait synthesis; Parametric optimisation; Spline-based parameterisation.

1. Introduction

Locomotion is the very basic task a biped robot must be able to perform. Unfortunately, the most likely natural behaviour a biped is prone to is to trip over, and to fall down. Thus, an essential problem to cope with for generating gait is to make compatible stable balance of the biped with efficient propulsive effects. More specifically, an appropriate coordination of joint movements is required while ensuring suitable contact interactions of feet on the supporting ground. These requirements can be fulfilled through the implementation of some organising principles able to generate stable walking. A variety of approaches were considered in order to obtain steady gait patterns.

The most surprising means to create bipedal walking consists of exploiting the pendulum-like behaviour a biped may exhibit spontaneously provided that its inertia distribution is compatible with some walking pace. Thus, it has been shown that bipeds with rigid or articulated legs can move steadily down a sloping ground using gravity as the only powering source.[1–3] The biped then performs as an inverted compound pendulum which combines alternative movements of the legs in a cyclic or nearly cyclic way. The related concept of passive-dynamics gait was originally due to McGeer,[4,5] and was revisited by a number of researchers.[6–9]

Passive bipeds cannot walk on level ground. However, for walking on flat floor, gravity can be used too as a simple means in order for the biped to organise its gait in a natural way. In that case, a minimum of actuation is required as there is no contribution of gravity to compensate for the energy expended during each step. Simple mechanical models of biped robots were designed so as to illustrate the principle of quasi-passive dynamic walking which results.[3,10,11] Both passive and quasi-passive walkers obey a natural organising principle due to pendulous effects resulting from gravity associated with a suitable mass distribution of the biped. Quasi-passive walking on level ground is made possible thanks to the fact that appropriate bipeds have non-dissipative joints allowing the legs to swing freely, only a few joints being actuated intermittently by applying quasi-impulsive driving torques. It should be emphasised that this type of on–off driving control has certain similarities to bang-off-bang control inputs which result from the minimum energy cost criterion implemented in the framework of the optimal control theory.[12]

There is a fundamental aspect of human walking quasi-passive bipeds cannot simulate which is an efficient control of ground-foot contact. Suitable active interactions with the supporting floor are essential for ensuring and restoring permanently the dynamic balance of the biped. The control of ground-foot interaction forces is also a means required to produce forward motion in such a way that the walking robot is able to go all over an assigned working area. Forces exerted on the ground are directly linked to the robot internal dynamics created by joint actuating torques. Consequently, there is the need for bipeds fully actuated.

Many bipedal robots were constructed over the previous decades. Especially, sophisticated humanoids[13–17] have been designed in recent years with the goal of mimicking human gait. Spontaneous regulation of walking due to pendulous effects must be substituted for a more general organisation principle possibly containing the former and offering the possibility of exerting an active control on footholds in order to gain in stability and agility of gait.

Controlling external interactions of the biped must be done by acting on its internal dynamics through joint actuating torques. In this respect, the basic concept put forwards is the zero-moment point criterion (ZMP) introduced by Vukobratovic.[18–20] The ZMP can be seen as defining the centre of pressure onto the footprints. Indeed, it has been used intensively as a dynamic balance indicator correlating the centre of pressure and the global dynamics of the biped. For this reason, the ZMP was employed as a means to control the biped and, as well, as a basic principle for generating the movement. This criterion associated with a measurement of ground-foot interaction forces was implemented successfully

* Corresponding author. E-mail: guy.bessonnet@orange.fr

to generate three-dimensional gait of humanoid bipeds.[21–26] Generally, this approach is associated with the simplified dynamics of the inverted pendulum model which considers the biped mass as lumped at the centre of inertia, and the ZMP as a mobile fulcrum for the pendulum.[26–31] An alternative use of the ZMP is proposed by Vukobratovic *et al.*[19] and defined as the semi-inverse method. It is based on prescribing predefined movements for the legs while generating a compensatory movement of the trunk in order for the ZMP to follow an appropriate trajectory. This approach was effectively used for generating stable gait.[32,33]

In the above techniques, the correlation between the contact conditions ensuring the dynamic balance of the biped and the motion dynamics created by the driving torques is noticeably simplified. As a result, the gait velocity compatible with this approach is limited.[24] In order to walk faster, the movement must be fully organised and the co-ordination of actuating efforts carried out accurately.

A consistent means to fulfil this requirement consists of achieving optimal dynamic synthesis of walking. In brief, this technique is based on extracting a solution of a dynamic model of the biped by minimising a performance criterion while satisfying a set of constraints featuring the gait pattern to be generated. This approach is appealing for two reasons. First, it does not require introducing any kinematic data through the step time. Second, it offers the possibility to satisfy efficiently all typical constraints of gait. In particular, ground interaction forces may be dealt with accurately in order to ensure adequate balance of the biped on its footholds. Moreover, the movements generated involve minimal amounts of joint powering torques together with reduced amounts of energy expended. As a consequence, the energetic autonomy of the biped could be increased significantly.

A variety of theoretical models and numerical techniques have been developed for generating optimal gait patterns. First, since movement optimisation of controlled mechanical systems falls logically into the scope of optimal control theory, the Pontryagin maximum principle (PMP) was used by some researchers.[34–37] Early, Chow and Jacobson[34] focused on developing necessary conditions for optimality set by the PMP when considering one leg reduced to only two body segments. More recently,[35,36] both single and double support phases of sagittal gait, together with starting and stopping steps were generated for a 7-link planar biped using the maximum principle. Both phases of gait were optimised separately not globally. In the latter case, the PMP would produce quite intricate optimality conditions resulting in a very complex multi-point boundary value problem.

Parametric optimisation techniques allow the difficulties raised by movements having multiple phases to be easily overcome. However, a number of models dealt with using parameterisation apply to the swing phase only of sagittal gait.[38–41] Configuration variables were approximated by polynomial functions defined on the overall motion time. This approach results in a small number of free parameters to be optimised. As a consequence, the computed solutions are weakly optimal. Parameterisation accuracy of the configuration variables can be drastically improved using spline functions which may be defined with a much higher number of shaping parameters than simple polynomial functions and with limited risk of unwanted oscillations generally produced by high-order polynomials. The spline approach was used to generate sagittal gait of a 7-link biped considering steps with a double support phase comprising two sub-phases.[42–44] Cyclic steps are optimised globally by minimising the integral quadratic amount of joint actuating torques. Denk and Schmidt[45] dealt with 3D-gait in a different way, by parameterising both the state variables and the control variables (i.e. joint actuating torques) and by minimising the integral amount of energy spent. Step length, step time together with sub-phase times are given. As the step is not globally optimised, this can give rise to unnecessarily high-joint accelerations.

In this paper, a dynamic synthesis method developed for generating 3D-gait is presented. The generating principle of gait is the minimisation of driving torques. A near minimum set of kinematic and sthenic constraints characterising the step sub-phases is defined so as to give the optimisation process more freedom to select an efficient movement. Especially, postural configurations and velocities at transition times between adjacent steps and sub-phases of the step considered are simultaneously optimised. Special attention is devoted to foot-ground interactions. In particular, the locations of the centres of pressure under each foot are accurately defined with respect to the movement dynamics in order to ensure a steady dynamic balance of the biped. A parametric optimisation technique is used to solve the primary optimal control problem which results. The method is based on using spline functions to approximate the configuration variables at control instants distributed along the motion time. The dynamic indeterminacy arising during the double support is solved through the parameterisation of constraint forces at front foot level.

The objective is to develop a computerised movement generator able to create fully organised steps provided with safe dynamics. Due to the huge amount of computation required by the optimisation process, the optimal dynamic synthesis method developed in the following sections is an off-line technique. The computed reference trajectories need moderate driving torques as well as little energy consumption. They could be implemented by the robot controller provided that a feedback stabiliser is able to compensate for potential disturbances as shown for instance by Plestan *et al.*[46], Djoudi *et al.*[47] and Kajita *et al.*[48]

Section 2 which follows is devoted to thorough kinematic and dynamic modelling of a generic walking step. In Section 3, a dynamic optimisation problem is summarised and the parametric optimisation technique used to solve it is developed. In Section 4, results of two gait simulations are presented. Concluding remarks are formulated in Section 5.

2. Gait Modelling

The models we intend to formulate are based on two main mechanical determinants of gait. The first is the kinematic architecture of the locomotion system, and the second is the way the feet develop their contact interactions with the ground.

https://doi.org/10.1017/S0263574709990257 Published online by Cambridge University Press

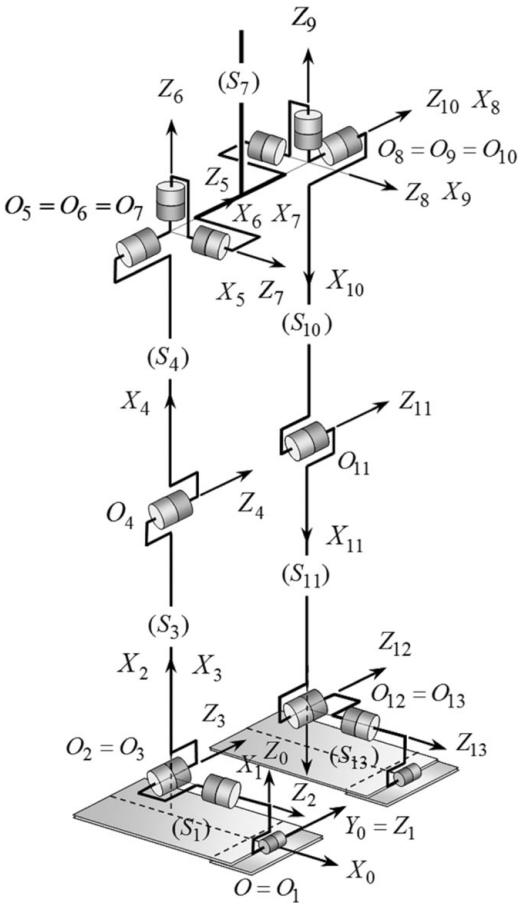

Fig. 1. Kinematic layout of the locomotion system comprising 12 actuated joints for the legs, plus two active joints in the feet. Setting up of joint axes $(O_i; Z_i)$, $i = 1, \ldots, 13$, related to Denavit–Hartenberg's construction (see Appendix A1).

2.1. Gait kinematics

Since we intend to generate three-dimensional walking, we consider a standard bipedal scheme as shown in Fig. 1. The three-link legs (foot, shin and thigh) have six internal degrees of freedom each: three at hip, one at knee and two at ankle. Humanoid robots[13–17] exhibit this minimal architecture needed to mimic human gait. As more recent bipeds such as Wabian-2R[16] and HRP-2LT[49] have toe joints, we account for an additional degree of freedom about the toe-joint axis ($(O_1; Z_1)$ in Fig. 1).

The basic kinematic cycle of gait is the step defined by two successive phases of single support and double support. The single support phase (SSP), or swing phase, goes from toe-off to heel-touch of the swing leg. The biped moves as an open tree-like kinematic chain. The double support phase (DSP) is initiated at heel-touch of the front foot, and ends at toeing-off of the rear foot. The locomotion system is then overactuated and moves as a closed kinematic chain.

Various sub-phases of the step can occur depending on whether the ground-foot interaction takes place at heel, along the sole, or at toe level. The most simple contact pattern is to consider that each foot remains flat on the ground throughout its contact phase. Such a configuration can help the biped to enhance its dynamic balance, therefore to make its gait safer. However, as the rear foot does not lever the leg up, the forward motion is weakened. In fact, this contact scheme is compatible with small steps and allows essentially for slow walking. More efficient gait patterns are the result of the movements of feet on the supporting floor when they can exert some lever effect on the ground before toeing off and after heel touch. A variety of contact patterns can be defined depending on the movements of the stance foot through the single support phase, together with the synchronisation of contact sub-phases of feet during the double support.[50] We have chosen to exemplify the following contact pattern: the stance foot remains flat on the ground through the SSP; then it rotates about its fore-foot axis during the DSP while the front foot first executes an heel-rocker movement during a beginning sub-phase labelled *DS*1 followed by an ending sub-phase *DS*2 with the foot in flat contact on the ground. Both sub-phases of the double support are illustrated in Fig. 2. Accordingly, the step duration is divided in three phases as shown in Fig. 3. Initial time t^i and final time t^f of the step cycle are also labelled t_0^* and t_3^*, respectively, while t_1^* and t_2^* are the transition times between single and double supports, and *DS*1, *DS*2 sub-phases.

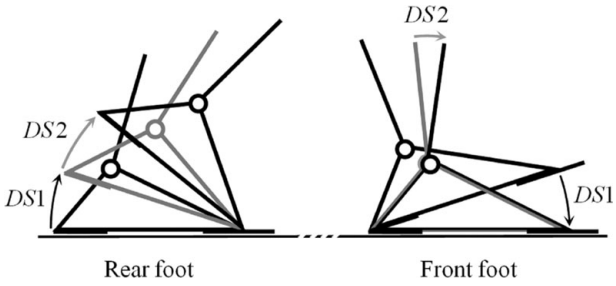

Fig. 2. Movements of the rear foot and front foot during the sub-phases *DS*1 and *DS*2 of the double support.

Considering the sequence SSP–DSP, one can observe that the toe-joint axis of the stance foot remains motionless throughout the step cycle. Thus, the biped may be regarded as a rooted kinematic chain, the stance foot (S_1) being its first moving link (Fig. 1). Consequently, the movement can be described by 13 joint coordinates q_i defined using the Denavit–Hartenberg construction[51] going from the link (S_1) to the swing foot (S_{13}), as detailed in Appendix 1.

2.1.1. Constraint equations. Joint coordinates q_is are not independent during the double support. As the front edge of the rear foot is considered as rooted, closure constraints for the kinematic chain must express that the front foot is in contact with the ground at the right place according to the contact pattern taken into account (Fig. 4). To begin with, a few specifications concerning the foot geometry must be defined. We assume that the feet have polygonal planar soles with parallel front and rear edges which are orthogonal to the

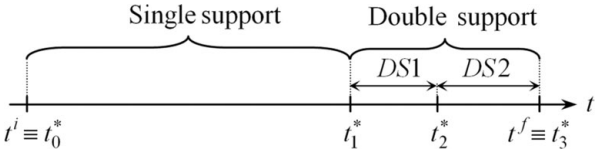

Fig. 3. Time slicing of the step cycle.

https://doi.org/10.1017/S0263574709990257 Published online by Cambridge University Press

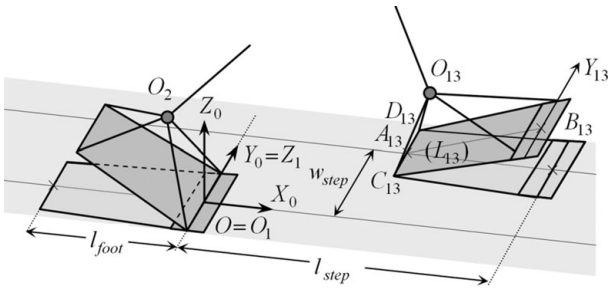

Fig. 4. Relative positioning of footprints and feet through the double support phase.

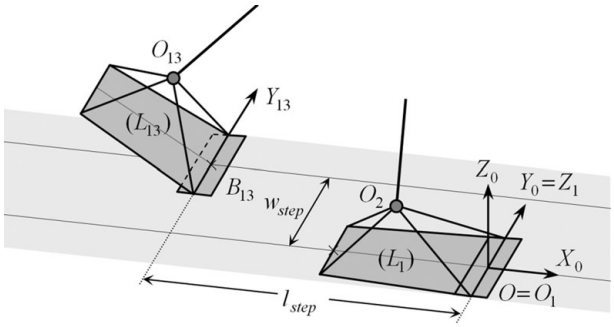

Fig. 5. Location of feet at initial time t_0^* of the single support.

foot median plane. This one is itself orthogonal to the sole and contains the ankle joint centre.

For the sake of simplicity and without lost of generality, we consider a step performed on flat floor, in a straight line as indicated in Fig. 4. Throughout the double support, the rear foot rotates about its toe joint axis ($(O; Y_0)$ in Fig. 4). The locomotion system closes in a kinematic loop on the forward footprint as shown in Fig. 4. During the first sub-phase $DS1$, the front foot rotates about its heel axis $(A_{13}; Y_{13})$. The related closure equations can be written as

$$k = 1, 2; t \in I^{DSk},$$
$$\begin{cases} \phi_1^{DSk}(q(t)) := OA_{13}(q(t)) \cdot X_0 - L_{\text{step}} + l_{\text{foot}} = 0 \\ \phi_2^{DSk}(q(t)) := OA_{13}(q(t)) \cdot Y_0 - w_{\text{step}} = 0 \\ \phi_3^{DSk}(q(t)) := OA_{13}(q(t)) \cdot Z_0 = 0 \end{cases}, \quad (1)$$

$$\begin{cases} \phi_4^{DSk}(q(t)) := Y_{13}(q(t)) \cdot Z_0 = 0 \\ \phi_5^{DSk}(q(t)) := -Y_{13}(q(t)) \cdot X_0 = 0 \end{cases}, \quad (2)$$

where q stands for the configuration vector $q = (q_1, \ldots, q_{13})^T$. l_{step} and w_{step} are the step length and width, and l_{foot} is the foot length.

The three first relationships in Eq. (1) express that the point A_{13} of the front foot is in its assigned location. Both following equations in Eq. (2) mean that the foot is kept in a proper orientation compatible with the heel-rocker movement.

During the second sub-phase $DS2$, the front foot is assumed to remain flat on the ground. This condition results in the further closure equation:

$$t \in I^{DS2}, \phi_6^{DS2}(q(t)) := -Z_{13} \cdot Z_0 = 0. \quad (3)$$

We summarise Eqs. (1)–(3) on each sub-phase by setting

$$t \in I^{DS1}, \Phi^{DS1}(q(t)) := (\phi_1^{DS1}(qt)), \ldots, \phi_5^{DS1}(q(t)) = 0 (\in \Re^5), \quad (4)$$

$$t \in I^{DS2}, \Phi^{DS2}(q(t)) := (\phi_1^{DS2}(qt)), \ldots, \phi_6^{DS2}(q(t)) = 0 (\in \Re^6). \quad (5)$$

2.1.2. Step initialising conditions. We must take into account conditions either initialising the step given a starting postural configuration, or expressing the movement continuity with the previous step. The latter case is illustrated in Fig. 5: at initial time t_0^*, the distal foot (S_{13}) takes off at front edge level (or equivalently, alongside the toe joint axis shown in Fig. 1). Five conditions express that the contact takes place along a straight line at toeing off:

$$\begin{cases} g_1^0(q(t_0^*)) := OB_{13}(q(t_0^*)) \cdot X_0 + L_{step} = 0 \\ g_2^0(q(t_0^*)) := OB_{13}(q(t_0^*)) \cdot Y_0 - l_{step} = 0 \\ g_3^0(q(t_0^*)) := OB_{13}(q(t_0^*)) \cdot Z_0 = 0 \end{cases}, \quad (6)$$

$$\begin{cases} g_4^0(q(t_0^*)) := Y_{13}(q(t_0^*)) \cdot X_0 = 0 \\ g_5^0(q(t_0^*)) := Y_{13}(q(t_0^*)) \cdot Z_0 = 0 \end{cases}. \quad (7)$$

These conditions are similar to the relationships (1) and (2) expressing the positioning of the heel edge $C_{13}D_{13}$ of the foot (S_{13}) during the double support.

Furthermore, the foot (S_{13}) toes off with a rotation velocity about its toe axis only. All other five velocity components of (S_{13}) considered as a free solid must be zero at time t_0^*. Thus, the following kinematic conditions are to be satisfied

$$\begin{cases} g_6^0(q(t_0^*), \dot{q}(t_0^*)) := V(B_{13}(q(t_0^*))) \cdot X_0 = 0 \\ g_7^0(q(t_0^*), \dot{q}(t_0^*)) := V(B_{13}(q(t_0^*))) \cdot Y_0 = 0, \\ g_8^0(q(t_0^*), \dot{q}(t_0^*)) := V(B_{13}(q(t_0^*))) \cdot Z_0 = 0 \end{cases} \quad (8)$$

$$\begin{cases} g_9^0(q(t_0^*), \dot{q}(t_0^*)) := \Omega(L_{13}(q(t_0^*))) \cdot Z_0 = 0 \\ g_{10}^0(q(t_0^*), \dot{q}(t_0^*)) := \Omega(L_{13}(q(t_0^*))) \cdot X_0 = 0 \end{cases}, \quad (9)$$

where $\dot{q}$ is the time derivative of the configuration vector q.

Conditions (8) (V is the velocity vector of point B_{13}) means that there is neither sliding velocity nor normal velocity of the foot at t_0^*. The condition (9) (Ω is the rotation velocity vector of the foot (S_{13})) indicates there is no rotation velocity about the directions defined by Z_0 and X_0. One can observe that relationships (8) and (9) could be derived from Eqs. (6) and (7) with respect to t_0^*. We put together the constraints (6)–(9) in the 10-vector constraint equation

$$g^0(q(t_0^*)) := (g_1^0(q(t_0^*)), \ldots, g_{10}^0(q(t_0^*)))^T = 0. \quad (10)$$

2.1.3. Constraints at transition times. The transition configurations $q(t_1^*)$ and $q(t_2^*)$ fulfil constraints imbedded in the closure equations formulated on the intervals I^{DS1} and I^{DS2}

https://doi.org/10.1017/S0263574709990257 Published online by Cambridge University Press

in Eqs. (6), (7) and (8). However, the transition states of the mechanical system must be completed by conditions preset on the velocities.

First, at t_1^*, the stance foot (S_1) is required to initiate a rotation about its leading edge without velocity break, hence with velocity equal to zero, which implies the condition

$$g_1^1(q(t_1^*), \dot{q}(t_1^*)) := \dot{q}_1(t_1^*) = 0. \tag{11}$$

At the same time, we assume that the swing foot (S_{13}) comes into contact with the ground without impact in order to avoid discontinuities of joint velocities which could be harmful for the biped and could disturb its control as shown by Blajer and Schielen.[52] This assumption results in the five equality constraints derived from the relationships (1) and (2):

$$g_{1+i}^1(q(t_1^*), \dot{q}(t_1^*)) := \left(\frac{\partial}{\partial q}\phi_i^{DS1}(q(t_1^*))\right)\dot{q}(t_1^*) = 0, \quad 1 \le i \le 5. \tag{12}$$

The first three ones mean that the velocity of the point A_{13} with respect to the ground is equal to zero. The two following signify there is no rotation velocity of the foot (S_{13}) about axes $(A_{13}; X_0)$ and $(A_{13}; Z_0)$ respectively. We bring together scalar constraints (11) and (12) in the vector constraint function $\mathbf{g}^1$ defined as

$$g^1(q(t_1^*), \dot{q}(t_1^*)) := (g_1^1(q(t_0^*), \dot{q}(t_1^*)), \ldots, g_6^1(q(t_0^*), \dot{q}(t_1^*)))^T = 0. \tag{13}$$

Second, at t_2^*, the sole of the foot (S_{13}) brings into flat contact. It could slam the ground. This situation is avoided if the rotation velocity of (S_{13}) about the heel edge $C_{13}D_{13}$ (Fig. 4) is zero. This condition can be formulated as the time derivative of closure Eq. (3) at t_2^*:

$$g_1^2(q(t_2^*), \dot{q}(t_2^*)) := \left(\frac{\partial}{\partial q}\phi_6^{DS2}(q(t_2^*))\right)\dot{q}(t_2^*) = 0. \tag{14}$$

2.1.4. Constraints at final time. Various situations may be considered. First, the step can be perfectly cyclic, the final state being deduced from the initial one by swapping the legs. Each $q_i(t_3^*)$ of the final configuration is then expressed explicitly as a function of the initial configuration $q(t_0^*)$. We write formally this condition as

$$g_i^3(q_i(t_3^*), q(t_0^*)) := q_i(t_3^*) - \varphi_i(q(t_0^*)) = 0, \quad 1 \le i \le 13. \tag{15}$$

In the same way, the final velocities must be derived from the initial ones. The corresponding constraints can be obtained as the time derivatives of the second part of Eq. (15)

$$g_{13+i}^3(\dot{q}_i(t_3^*), q(t_0^*), \dot{q}(t_0^*)) := \dot{q}_i(t_3^*) - \left(\frac{\partial}{\partial q}\varphi_i(q(t_0^*))\right)\dot{q}(t_0^*) = 0. \tag{16}$$

We assemble the scalar constraints (15) and (16) in the vector function

$$g^3(\dot{q}_i(t_3^*), q(t_0^*), \dot{q}(t_0^*)) := (g_1^3(\dot{q}_i(t_3^*), q(t_0^*)), \ldots, g_{26}^3(\dot{q}_i(t_3^*), q(t_0^*), \dot{q}(t_0^*))) = 0. \tag{17}$$

Dependency between initial and final states may disappear or be reduced if one considers starting or stopping steps, upward or downward steps (on horizontal supporting surfaces), or else turning steps. In such cases, a final state must be specified, with or without dependency with respect to the initial state. In the following, we consider purely cyclic steps to illustrate our optimal synthesis approach. This is the most constrained case among various feasible step cycles. It is also the means to generate fast steady gait. It should be added that the method implemented offers the possibility to achieve numerical simulations of a variety of other gait patterns.

2.2. Gait dynamics

As emphasised in Section 1, a key factor in succeeding to generate and control efficiently stable gait is to correlate accurately internal control inputs with external interaction forces exerted by the biped on the supporting ground. This correlation is defined by a dynamic model of the biped based on a relevant inertial model. Generally, the inverse dynamic approach is used both for generating and controlling the movement. This is also the choice required by the dynamic synthesis method we intend to develop in Section 3.

2.2.1. Inverse dynamic modeling. Since we have assumed that all joints are actuated, each configuration variable q_i is associated with an actuating torque τ_i, $i = 1, \ldots, 13$. It should be noticed that the toe joint of the swing foot/front foot (S_{13}) is considered as idle throughout the step sequence. Moreover, we assume that the toe joint of the stance foot (S_1) is locked through the SSP. Thus, as q_1 remains constant while τ_1 is zero, a reduced configuration q^r can be used to formulate the Lagrangian dynamic model of the single support as the 12-dimensional vector equation:

$$t \in I^{\mathrm{SSP}}, \quad M(q^r)\ddot{q}^r + H(q^r, \dot{q}^r) = \tau^r, \tag{18}$$

where $q^r = (q_2^r, \ldots, q_{13}^r)^T$, $\tau^r = (\tau_2^r, \ldots, \tau_{13}^r)^T$, M is the mass matrix of the biped in its reduced configuration, and the vector function H groups Coriolis, centrifugal and gravity terms together.

Considering the inverse dynamic problem, Eq. (18) indicates explicitly that actuating torques are functions of the configuration vector q^r and its time derivatives, which can be formally written as

$$t \in I^{\mathrm{SSP}}, \quad \tau_i^r = T_i(q^r, \dot{q}^r, \ddot{q}^r),\ i = 2, \ldots, 13. \tag{19}$$

During the double support, the full configuration vector q complies with constraint Eqs. (4) and (5). The Lagrangian model is then defined as the 13-dimensional vector equation over each sub-phase $DS1$ and $DS2$:

$$t \in I^K, \quad K \in \{DS1, DS2\}, \quad M(q)\ddot{q} + H(q, \dot{q}) = \tau + (J^K(q))^T\lambda^K, \tag{20}$$

https://doi.org/10.1017/S0263574709990257 Published online by Cambridge University Press

where $J^K = \frac{\partial \Phi^K}{\partial q}$ is the Jacobian matrix of the closure constraint Φ^K as defined in Section 2.1.1, and λ^K is the associated Lagrange's multiplier which assembles the components of forces to be applied to the front foot in order to keep it in its assigned position. Labelling F_{13}^K and $M^K(A_{13})$ the resultant and the moment at point A_{13} of forces exerted by the ground on the foot (S_{13}) throughout the double support ($K \in \{DS1, DS2\}$), the components of λ^K can be swiftly identified as

$$K \in \{DS1, DS2\},$$

$$\begin{cases} \lambda_1^K = F_{13}^K \cdot X_0 \\ \lambda_2^K = F_{13}^K \cdot Y_0 \\ \lambda_3^K = F_{13}^K \cdot Z_0 \\ \lambda_4^K = M^K(A_{13}) \cdot X_0 \\ \lambda_5^K = M^K(A_{13}) \cdot Z_0 \end{cases}, \lambda_6^{DS2} = M^{DS2}(A_{13}) \cdot Y_0. \quad (21)$$

Equation (20) results in an inverse dynamic problem exhibiting 18 or 19 unknowns (13 τ_is plus 5 or 6 λ_j^Ks through the sub-phases $DS1$ and $DS2$ respectively). This under-determined algebraic linear system can be solved using a pseudo-inversion. Such an operation amounts to extracting a minimal morn solution in τ and λ^K. This technique has been applied for generating optimal gait cycles of planar bipeds.[42–44] In the following (Section 3), we consider another approach which consists of approximating the λ_j^Ks (as well as the q_is) by parameterised functions defined as explicit time functions. In this way, only the τ_is remains as unknown time functions then defined through Eq. (20) as

$$t \in I^K, K \in \{DS1, DS2\}, \tau_i = T_i(q, \dot{q}, \ddot{q}, \lambda^K), \quad i = 2, \ldots, 13. \quad (22)$$

A thorough calculation of functions T_is in Eqs. (19) and (22) is required by the optimisation method developed in Section 3. It could be done using a full formulation of Eqs. (18) and (20). However, computation of Lagrange's equations is lengthy and time consuming. The parameterisation of the λ_j^Ks amounts to dealing with the contact forces at front foot as given input variables in the optimisation process. Therefore, it becomes possible to compute the actuating torques τ_is more directly with the Newton–Euler equations using the well known Luh, Walker and Paul method.[51] This approach has also the advantage of computing directly the contact forces on the stance foot at the end of the backward recursion. Thus, the resultant F_1^K and the moment $M^K(O_1)$ at O_1 of forces exerted by the ground on the foot (S_1) appear as functions of $q, \dot{q}, \ddot{q}$, and $\tau(q, \dot{q}, \ddot{q})$ through the single support, and as functions of the sequence of variables $q, \dot{q}, \ddot{q}, \lambda^K$ and $\tau(q, \dot{q}, \ddot{q}, \lambda^K)$ through the double support. Therefore, they are functions of the primary variables $q, \dot{q}, \ddot{q}, \lambda^K$ as follows:

$$\begin{cases} K = \text{SSP}, \begin{cases} F_1^K = F_1^K(q, \dot{q}, \ddot{q}) \\ M_1^K = M_1^K(q, \dot{q}, \ddot{q}) \end{cases} \\ K \in \{DS1, DS2\}, \begin{cases} F_1^K = F_1^K(q, \dot{q}, \ddot{q}, \lambda^K) \\ M_1^K = M_1^K(q, \dot{q}, \ddot{q}, \lambda^K) \end{cases} \end{cases}. \quad (23)$$

In order to ensure that each foot keeps its ground supports stable, the contact forces defined in Eqs. (21) and (23) must be subjected to a suitable set of constraints described in the following section.

2.2.2. Constraining contact forces. Contact forces exerted by the ground on the feet must satisfy conditions such as unilaterality of contact, non-sliding of the feet on the ground and balance safeguarding of the biped on its ground supports.

2.2.2.1. Unilaterality and non-sliding constraints. Unilaterality of contact is expressed by the positivity of the normal component of the resultant of forces exerted by the ground on each foot. We assume that ground-foot friction is of Coulombian type and account for translatory sliding only. Considering, first, the single support, both above conditions take the form

$$K = \text{SSP}, \begin{cases} F_1^K \cdot Z_0 > 0 \\ \left\| F_1^K - (F_1^K \cdot Z_0) Z_0 \right\| < f_1 (F_1^K \cdot Z_0) \end{cases}$$

where the factor f_1 is a dry friction coefficient. Through the dependency shown in Eq. (23) for F_1^K, they define constraint functions we write as

$$\begin{cases} h_1^{1\text{SSP}}(q, \dot{q}, \ddot{q}) := -F_1^{\text{SSP}} \cdot Z_0 < 0 \\ h_1^{2\text{SSP}}(q, \dot{q}, \ddot{q}) := \left\| F_1^{\text{SSP}} - (F_1^{\text{SSP}} \cdot Z_0) Z_0 \right\| \\ \quad - f_1 (F_1^{\text{SSP}} \cdot Z_0) < 0 \end{cases} \quad (24)$$

Similar constraints for the double support result in the following constraint functions defined accounting for the dependency appearing in Eqs. (21) and (23):

$$K \in \{DS1, DS2\},$$

$$\begin{cases} \begin{cases} h_1^{1K}(q, \dot{q}, \ddot{q}, \lambda^K) := -F_1^K \cdot Z_0 < 0 \\ h_1^{2K}(q, \dot{q}, \ddot{q}, \lambda^K) := \left\| F_1^K - (F_1^K \cdot Z_0) Z_0 \right\| \\ \quad - f_1 (F_1^K \cdot Z_0) < 0 \end{cases} \\ \begin{cases} h_{13}^{1K}(\lambda^K) := -F_{13}^K \cdot Z_0 < 0 \\ h_{13}^{2K}(\lambda^K) := \left\| F_{13}^K - (F_{13}^K \cdot Z_0) Z_0 \right\| \\ \quad - f_{13} (F_{13}^K \cdot Z_0) < 0 \end{cases} \end{cases}. \quad (25)$$

2.2.2.2. CoP/ZMP constraints. It should be emphasised that the notion of one-sided contact leads to the concept of *centre of pressure* (CoP) (or zero moment point: ZMP) which allows the dynamic balance of the biped to be dealt with efficiently. Considering a ground-foot contact area, the centre of pressure is characterised by the fact that the moment of normal forces at this point is zero.[18–20,53] Therefore, the moment of full contact forces at the CoP is normal to the supporting surface. Correlatively, the tipping moment of the foot at this point is equal to zero. Thus, it may be said that the closer to the geometric centre of the footprint the CoP is, the more secure the foothold is (provided that non sliding conditions are satisfied simultaneously). Conversely, if the CoP is situated on an edge of the footprint, the balance of the foot on its support is at risk. In this situation, the force distribution can be modified, that is to say controlled, only along the edge. The foot is then in a position to tip over its edge.

https://doi.org/10.1017/S0263574709990257 Published online by Cambridge University Press

One can consider that the CoP is a balance centre for the contact forces on the footprint. Particularly, the CoP should be kept inwards from the lateral hedges in order to avoid the lost of control of the lateral balance of the biped.

The location of the centre of pressure is defined by the formula (A2.2) given in Appendix 2. Both centres of pressure C_1^K and C_{13}^K of the feet (S_1) and (S_{13}) can be positioned on their assigned footprints by vector functions Ψ_1^K and Ψ_{13}^K defined through the relationship (A2.2) and the formulations (21) and (23) as follows:

$$O_1C_1^K = \frac{Z_0 \times M_1^K(O_1)}{Z_0 \cdot F_1^K} := \begin{cases} \Psi_1^K(q, \dot{q}, \ddot{q}) \text{ if } K = \text{SSP} \\ \Psi_1^K(q, \dot{q}, \ddot{q}, \lambda^K) \text{ if } K \in \{DS1, DS2\} \end{cases}, \quad (26)$$

$$A_{13}C_{13}^K = \frac{Z_0 \times M_{13}^K(A_{13})}{Z_0 \cdot F_{13}^K} := \Psi_{13}^K(\lambda^K), \quad K \in \{DS1, DS2\}. \quad (27)$$

In order for each CoP to be in its assigned footprint, its coordinates must satisfy geometrical limitations. Two cases must be distinguished according to the CoP is either inside the convex polygonal outline or on an edge of the footprint. In Fig. 6, (X_k, Y_k) and (X, Y) are the Cartesian coordinates in the local frame $(O; X_0, Y_0, Z_0)$ of the vertex E^k $(1 \leq k \leq n_E)$ and the inside point C, respectively. The point C is inside the polygon if its projection onto the inward normal to each edge is situated inwards. Considering E^kE^{k+1} in Fig. 6, this normal is parallel to the vector $Z_0 \times E^kE^{k+1}$ $(Z_0 = X_0 \times Y_0)$. Thus, the required condition is expressed as the inequality

$$1 \leq k \leq n_E, E^kC \cdot (Z_0 \times E^kE^{k+1}) > 0.$$

This condition defines the following n_E constraint functions

$$f_k(X, Y) := (Y_{k+1} - Y_k)(X_k - X) - (X_{k+1} - X_k)(Y_k - Y) < 0. \quad (28)$$

If C is situated on an edge, for instance E^kE^{k+1}, a first condition to be satisfied is that both vectors E^kC and E^kE^{k+1} are parallel, that is to say $E^kC \times E^kE^{k+1} = 0$. This condition

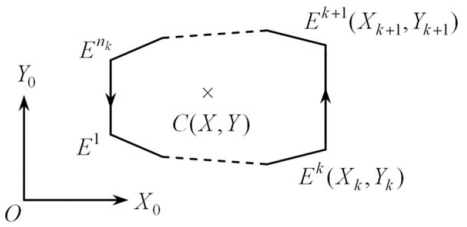

Fig. 6. Oriented polygonal outline of a generic footprint and its centre of pressure C.

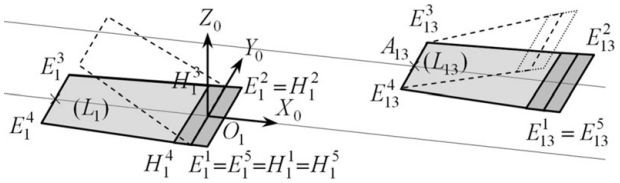

Fig. 7. Polygonal outlines $E_1^1E_1^2E_1^3E_1^4$, $H_1^1H_1^2H_1^3H_1^4$ and $E_{13}^1E_{13}^2E_{13}^3E_{13}^4$ of the footprints during the step considered.

can be expressed as the only constraint function

$$g_k(X, Y) := (Y_{k+1} - Y_k)(X_k - X) - (X_{k+1} - X_k)(Y_k - Y) = 0. \quad (29)$$

Moreover, C must be situated between the points E^k and E^{k+1}, which results in both inequalities

$$0 < E^kC \cdot E^kE^{k+1} < l_k,$$

where $l_k = \|E^kE^{k+1}\|$.

If we let

$$h_k(X, Y) := E^kC \cdot E^kE^{k+1} = (X_{k+1} - X_k)(X_k - X) - (Y_{k+1} - Y_k)(Y_k - Y) = 0.$$

the above double inequality takes the form of the two constraints

$$\begin{cases} -h_k(X, Y) < 0 \\ h_k(X, Y) - l_k < 0 \end{cases}. \quad (30)$$

Formulae (28), (29) and (30) must be applied to the footprints represented in Fig. 7. It should be noticed that the coordinates (X_1^K, Y_1^K) and (X_{13}^K, Y_{13}^K) of points C_1^K and C_{13}^K have the type of dependency given in relationships (26) and (27). Both main phases are dealt with one by one.

Single support

The foot (S_1) is flat. The centre of pressure is in its assigned footprint $E_1^1 \ldots E_1^4$ if the following four constraints of type (28) are satisfied

$$h_{1k}^{\text{SSP}}(q, \dot{q}, \ddot{q}) := f_k(X_1^{\text{SSP}}(q, \dot{q}, \ddot{q}), Y_1^{\text{SSP}}(q, \dot{q}, \ddot{q})) < 0, \quad 1 \leq k \leq 4. \quad (31)$$

Double support

The footprint for C_1^K is the quadrilateral surface $H_1^1 \ldots H_1^4$ (Fig. 7) throughout the double support. The constraints to be accounted for are similar to the previous ones in Eq. (31); however, with the dependency given in Eq. (26). Therefore, we have, for $K \in \{DS1, DS2\}$:

$$h_{1k}^K(q, \dot{q}, \ddot{q}, \lambda^K) := f_k(X_1^K(q, \dot{q}, \ddot{q}, \lambda^K), Y_1^K(q, \dot{q}, \ddot{q}, \lambda^K)) < 0, 1 \leq k \leq 4. \quad (32)$$

During the first sub-phase $DS1$, the front foot is in contact along its heel edge $E_{13}^3E_{13}^4$. The centre of pressure C_{13}^{DS1} is

https://doi.org/10.1017/S0263574709990257 Published online by Cambridge University Press

then subjected to constraints of type (29) and (30) with the dependency of X_{13}^{DS1} and Y_{13}^{DS1} given in Eq. (27):

$$\begin{cases} g_{13}^{DS1}(\lambda^{DS1}) := g_3\big(X_{13}^{DS1}(\lambda^{DS1}), Y_{13}^{DS1}(\lambda^{DS1})\big) = 0 \\ h_{13,1}^{DS1}(\lambda^{DS1}) := -h_3\big(X_{13}^{DS1}(\lambda^{DS1}), Y_{13}^{DS1}(\lambda^{DS1})\big) < 0 \\ h_{13,2}^{DS1}(\lambda^{DS1}) := h_3\big(X_{13}^{DS1}(\lambda^{DS1}), Y_{13}^{DS1}(\lambda^{DS1})\big) - l_3 < 0 \end{cases}. \tag{33}$$

The foot (L_{13}) is flat on the ground through the second sub-phase $DS2$. Therefore, the coordinates X_{13}^{DS2} and Y_{13}^{DS2} are limited by four constraints of type (28) as follows:

$$h_{13,k}^{DS2}(\lambda^{DS2}) := f_k(X_{13}^{DS2}(\lambda^{DS2}), Y_{31}^{DS2}(\lambda^{DS2})) < 0, 1 \le k \le 4. \tag{34}$$

2.3. Technological and anti-collision constraints

State variables q_is and $\dot{q}_i$s together with joint actuating inputs τ_is must be subjected to restrictions corresponding to technological capabilities of the walking robot. These limitations result in box constraints such as

$$t \in I^{step}, 1 \le i \le n_q, \begin{cases} h_i^{q,\min}(q(t)) := -q_i(t) + q_i^{\min} \le 0 \\ h_i^{q,\max}(q(t)) := q_i(t) - q_i^{\max} \le 0 \\ h_i^{\dot{q},\min}(\dot{q}(t)) := -\dot{q}_i(t) + \dot{q}_i^{\min} \le 0 \\ h_i^{\dot{q},\max}(\dot{q}(t)) := \dot{q}_i(t) - \dot{q}_i^{\max} \le 0 \\ h_i^{\tau,\min}(\tau(t)) := -\tau_i(t) + \tau_i^{\min} \le 0 \\ h_i^{\tau,\max}(\tau(t)) := \tau_i(t) - \tau_i^{\max} \le 0 \end{cases}. \tag{35}$$

Limitations imposed on the q_is are essential in order for the robot to avoid odd configurations such as, for instance, hyperextensions at knees and ankles. We assemble the constraints set on the q_is and $\dot{q}_i$s into the two $2n_q$-vector constraint functions:

$$t \in I^{step}, \begin{cases} h^q(q(t)) := (h_1^{q,\min}, h_1^{q,\max}, \ldots, h_{n_q}^{q,\min}, h_{n_q}^{q,\max})^T \\ \quad \le 0 (\in \Re^{2n_q}) \\ h^{\dot{q}}(q(t)) := (h_1^{\dot{q},\min}, h_1^{\dot{q},\max}, \ldots, h_{n_q}^{\dot{q},\min}, h_{n_q}^{\dot{q},\max})^T \\ \quad \le 0 (\in \Re^{2n_q}) \end{cases}. \tag{36}$$

Similarly, setting for the τ_is: $h^\tau = (h_1^{\tau,\min}, h_1^{\tau,\max} \ldots, h_{n_q}^{\tau,\min}, h_{n_q}^{\tau,\max})^T$, then the vector-constraint

$$t \in I^{step}, h^\tau(\tau(t)) \le 0 (\in \Re^{n_q}),$$

will be used with the dependency given in Eqs. (21) and (22):

$$\begin{cases} t \in I^{\mathrm{SSP}}, h^{\tau,\mathrm{SSP}}(q, \dot{q}, \ddot{q}) := h^\tau(\tau(q, \dot{q}, \ddot{q})) \le 0 \\ t \in I^K, K \in \{DS1, DS2\}, \\ \quad h^{\tau,K}(q, \dot{q}, \ddot{q}, \lambda^K) := h^\tau(\tau(q, \dot{q}, \ddot{q}, \lambda^K)) \le 0 \end{cases}. \tag{37}$$

Configuration variables q_is have to satisfy further constraints defined so as to protect the biped against collisions. First, internal collisions between the legs must be avoided through the single support. During normal walking, that is to say performed without exaggerated gesticulating, body segments (S_{11}) and (S_{13}) of the swing leg are likely to collide with their stance leg counterparts (S_1) and (S_3). We assume that there is neither unnecessary adduction–abduction movement of the foot (S_{13}) about its frontal axis ($O_{13}; Z_{13}$) nor exaggerated internal–external rotation of the swing leg at hip. In such a case, keeping the axis ($O_{11}; X_{11}$) of the swing leg to an adequate minimal distance $\delta^{\min}$ from the axis ($O_3; X_3$) of the stance leg may be considered as a satisfactory non-colliding condition which can be written as

$$t \in I^{\mathrm{SSP}}, h^{ica}(q(t)) := -\delta(q(t)) + \delta^{\min} \le 0 (\in \Re), \tag{38}$$

where the function $\delta(q(t))$ is the distance between both axis at current time t.

Furthermore, the swing foot could hit the ground or an obstacle. In order to avoid such external collisions the foot must be kept at adequate clearance distance. We adopted a simple technique for external collision avoidance described in Marot.[50] It results in constraints we write formally as

$$t \in I^{\mathrm{SSP}}, h^{eca}(q(t)) \le 0 (\in \Re^{n_{eca}}). \tag{39}$$

3. Dynamic Synthesis of Gait

Dynamic synthesis of movement is achieved by computing an optimal feasible solution for the dynamic equations of the mechanical system, that is to say a solution which minimises a performance criterion and fulfils constraints characterising the movement to be generated. A set of such constraints has been detailed in the previous section. A performance criterion must be defined and a solving method is required to compute appropriate solutions.

3.1. Performance criterion

In the field of dynamic optimisation, two basic criteria are at issue. First, an energetic criterion is generally defined as the integral of absolute joint actuating powers over the motion time.[39–41,45] It must be underlined that the minimum-energy cost produces bang-off-bang actuating inputs, that is to say optimal powering torques switching between finite sub-intervals of time from the zero value to given extremal bounds.[12] Such non-smooth variations can be attenuated when implementing a parametric optimisation technique. However, unnecessary high joint accelerations may be generated.[45]

Another widespread criterion is the minimum-effort cost[35–37,54] defined as the integral of quadratic actuating torques. We have chosen to implement this criterion considering its value per unit of distance covered as follows

$$C_\tau = \frac{1}{l_{\mathrm{step}}} \int_{t^i}^{t^f} \sum_{i=1}^{13} \xi_i \tau_i(t)^2 \, \mathrm{d}t, \tag{40}$$

where ξ_is are weighting factors equal or close to one. This criterion yields smooth optimal inputs. Furthermore, it has

https://doi.org/10.1017/S0263574709990257 Published online by Cambridge University Press

proved to be particularly appropriate for generating gait[43,44] due to the fact that it tends to produce upright walking in order for the joint torques to be subjected to moderate effects of the biped weight. Dividing the integral by l_{step} will allow the step length to be efficiently optimised versus a given walking velocity.

In the optimisation process (Section 3.2), the τ_is will be dealt with as functions of type (19) and (22). Thus, the formulation (40) turns into the relationship

$$C_\tau = \frac{1}{l_{\text{step}}} \sum_{i=1}^{13} \xi_i \left(\int_{t^i}^{t_1^*} T_i^2(q^r(t), \dot{q}^r(t), \ddot{q}^r(t))\, \mathrm{d}t + \sum_{k=1,2} \int_{t_k^*}^{t_{k+1}^*} T_i^2(q(t), \dot{q}(t), \ddot{q}(t), \lambda^{DSk}(t))\, \mathrm{d}t \right), \quad (41)$$

where $T_1(q^r, \dot{q}^r, \ddot{q}^r) = 0$ (Section 2.2.1).

It must be emphasise that the transition from Eq. (40) to Eq. (41) is the result of solving the movement equations using an inverse dynamic process. Thus, through the formulation (41), these equations disappear from the set of constraints remaining to be satisfied.

At this point, the problem to be solved consists of determining unknown functions $q(t)$ and $\lambda^{DSk}(t)$ minimising the criterion (41) and satisfying the constraints defined in Section 2. In the next section, the determination of these functions is carried out using a parametric optimisation technique.

3.2. Parametric optimisation

Various methods can be used for converting a dynamic optimisation or optimal control problem into a parametric optimisation problem. The reader is referred to Hull[55] and Betts[56] for a general presentation of techniques commonly employed to achieve such transformations.

The approach implemented in this paper is based on approximating the unknown functions $q_i(t)$ and $\lambda_j^{DSk}(t)(k = 1, 2)$ by specified time functions depending on a finite set of shaping parameters which are intended to be optimised in the resulting parametric optimisation problem. We have chosen to implement spline-functions built up as the concatenation of polynomials defined over sub-intervals of the cycle time and connected at knots uniformly distributed over each step sub-phase as shown in Fig. 8).

3.2.1. Parameterising the configuration variables. The q_is must be twice differentiable over each sub-phase of the step cycle. Thus, concatenating 3-order polynomials in order to obtain splines of class C^2 is sufficient to fulfil this requirement.[42] Nevertheless, in this case, as mentioned in Seguin and Bessonnet[43] and Bessonnet *et al.*,[44] joint accelerations may have angular variations at knots resulting in jerky movements. As in the last two references, we have introduced C^3-splines in order to generate smooth movements. These approximating functions are obtained by concatenating 4-order polynomials we define as follows

$$K \in \{\text{SSP}, DS1, DS2\}, 1 \le j \le N_K, \begin{cases} t \in \left[t_j^K, t_{j+1}^K\right], \bar{t} = \left(t - t_j^K\right)/\left(t_{j+1}^K - t_j^K\right) (\in [0, 1]), \\ q_i(t) \approx P_{ij}^K(\bar{t}) := a_{ij}^K + b_{ij}^K \bar{t} + c_{ij}^K \bar{t}^2 + d_{ij}^K \bar{t}^3 + e_{ij}^K \bar{t}^4 \end{cases}, \quad (42)$$

and connect at inner knots up to the third order:

$$K \in \{\text{SSP}, DS1, DS2\}, 2 \le j \le N_K, \begin{cases} P_{i,j-1}^K(1) = P_{ij}^K(0) \\ \dot{P}_{i,j-1}^K(1) = \dot{P}_{ij}^K(0) \\ \ddot{P}_{i,j-1}^K(1) = \ddot{P}_{ij}^K(0) \\ \dddot{P}_{i,j-1}^K(1) = \dddot{P}_{ij}^K(0) \end{cases}. \quad (43)$$

Moreover, the assumption of impactless movement at transition times t_1^* ($t_1^* \equiv t_{N_{\text{SSP}}+1}^{\text{SSP}} = t_1^{DS1}$, see Fig. 8) and t_2^* ($t_2^* \equiv t_{N_{DS1}+1}^{DS1} = t_1^{DS2}$) requires prescribing the continuity of the q_is and $\dot{q}_i$s as follows

$$\begin{aligned} &\text{At } t_1^*, \begin{cases} P_{i,N_{\text{SSP}}}^{\text{SSP}}(1) = P_{i,1}^{DS1}(0) \\ \dot{P}_{i,N_{\text{SSP}}}^{\text{SSP}}(1) = \dot{P}_{i,1}^{DS1}(0) \end{cases} \\ &\text{At } t_2^*, \begin{cases} P_{i,N_{DS1}}^{DS1}(1) = P_{i,1}^{DS2}(0) \\ \dot{P}_{i,N_{DS1}}^{DS1}(1) = \dot{P}_{i,1}^{DS2}(0) \end{cases} \end{aligned}. \quad (44)$$

In addition, the values $q_i(t_j^K)$ at all knots will be dealt with as shaping parameters to be optimised. They must be explicitly assigned to the polynomials P_{ij}^K:

$$\begin{cases} K \in \{\text{SSP}, DS1, DS2\}, 1 \le j \le N_K, P_{i,j}^K(0) = q_i\left(t_j^K\right) \\ P_{i,N_{DS2}}^{DS2}(1) = q_i(t^f), \left(t^f \equiv t_{N_{DS2}+1}^{DS2}\right) \end{cases}. \quad (45)$$

In the same way, the generalised velocities $\dot{q}_i$s will be considered as further optimisation variables at initial and final times, and at transition times, which results in the new assignment relationships

$$\begin{cases} \dot{P}_{i,1}^{\text{SSP}}(0) = \dot{q}_i(t^i), \quad \left(t^i \equiv t_1^{\text{SSP}}\right) \\ \dot{P}_{i,1}^{DS1}(0) = \dot{q}_i(t_1^*), \quad \left(t_1^* \equiv t_1^{DS1}\right) \\ \dot{P}_{i,1}^{DS2}(0) = \dot{q}_i(t_2^*), \quad \left(t_2^* \equiv t_1^{DS2}\right) \\ \dot{P}_{i,N_{DS2}}^{DS2}(1) = \dot{q}_i(t^f), \quad \left(t^f \equiv t_{N_{DS2}+1}^{DS2}\right) \end{cases}. \quad (46)$$

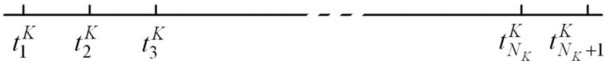

Fig. 8. Time slicing and connecting knots over any sub-phase K, $K \in \{\text{SSP}, DS1, DS2\}$.

In accordance with the notations in Fig. 8, for every subscript i, the number N of interpolating polynomials in (42) is defined by the equality $N = N_{\text{SSP}} + N_{DS1} + N_{DS2}$. Thus, we create the $(N + 5)$-vector of shaping parameters

https://doi.org/10.1017/S0263574709990257 Published online by Cambridge University Press

for the spline function approximating q_i:

$$\begin{aligned} X^i = & \left(x_1^i, \ldots x_{N+5}^i\right)^T \\ := & \left(\dot{q}_i\left(t_1^{\mathrm{SSP}}\right), q_i\left(t_1^{\mathrm{SSP}}\right), q_i\left(t_2^{\mathrm{SSP}}\right), \ldots, q_i\left(t_{N_{SA}}^{\mathrm{SSP}}\right)\right. \\ & \dot{q}_i\left(t_1^{DS1}\right), q_i\left(t_1^{DS1}\right), q_i\left(t_2^{DS1}\right), \ldots, q_i\left(t_{N_{DS1}}^{DS1}\right). \\ & \dot{q}_i\left(t_1^{DS2}\right), q_i\left(t_1^{DS2}\right), q_i\left(t_2^{DS2}\right), \ldots, q_i\left(t_{N_{DS2}}^{DS2}\right) \\ & \left. q_i(t^f), \dot{q}_i(t^f)\right)^T \end{aligned} \quad (47)$$

As one can easily see, relationships (43)–(46) represent $5N-3$ equations to be satisfied by the $5N$ polynomial coefficients introduced in Eq. (42) for q_i. In order to eliminate these coefficients versus the shaping parameters using above equations, their number must be reduced exactly to $5N-3$. This can be done by considering three 3-degree polynomials defined, for example, on the first sub-interval of each step phase. In this way, q_i is approximated by a spline function ϕ_i depending on the $(N+5)$-order vector X^i such as

$$t \in I_{\mathrm{step}}, q_i(t) \approx \phi_i(X^i, t), 1 \leq i \leq n_q. \quad (48)$$

Now, setting

$$\begin{aligned} X &= ((X^1)^T, \ldots, (X^i)^T, \ldots, (X^{n_q})^T)^T, \quad (49) \\ \phi(X,t) &= (\phi_1(X^1,t), \ldots, \phi_{n_q}(X^{n_q},t))^T, \end{aligned}$$

the configuration vector q is approximated as required

$$t \in I_{\mathrm{step}}, q(t) \approx \phi(X,t). \quad (50)$$

The order N_X of the vector X of shaping parameters for the q_is is expressed by the formula

$$N_X = n_q(N+5). \quad (51)$$

3.2.2. Parameterising the contact forces $\boldsymbol{\lambda^K}$. In the inverse dynamic scheme presented in Section 2.1.1, we consider the components of the wrench $\lambda^K (K \in \{DS1, DS2\})$ of contact forces exerted by the ground on the front foot as primary variables to be parameterised. The components λ_j^K can be subjected to discontinuities at transition times t_1^* and t_2^*. Consequently, they must be dealt with separately over the sub-phases $DS1$ and $DS2$. Moreover, they are assumed to vary continuously through each sub-phase. As a result, concatenating first-order polynomials, which yields splines of class C^0, offers a sufficient level of smoothness for approximating the λ_j^Ks.

Thus, if we set

$$\left.\begin{array}{l} K = DS1, 1 \leq j \leq 5, \\ K = DS2, 1 \leq j \leq 6 \end{array}\right\} Y^{K,j} = \left(\lambda_j^K(t_1^K), \ldots, \lambda_j^K(t_{N_K+1}^K)\right)^T,$$

next, defining

$$\left\{\begin{array}{l} Y^{DS1} = ((Y^{DS1,1})^T, \ldots, (Y^{DS1,5})^T)^T \\ Y^{DS2} = ((Y^{DS2,1})^T, \ldots, (Y^{DS2,6})^T)^T \end{array}\right.,$$

and following an approach similar to the technique developed in Section 3.2.1, one can approximate λ^K by a continuous vector-spline function ψ^K such as

$$K \in \{DS1, DS2\}, t \in I^K, \lambda^K(t) \approx \psi^K(Y^K, t). \quad (52)$$

Finally, setting

$$Y = ((Y^{DS1})^T, (Y^{DS2})^T)^T, \quad (53)$$

the number N_Y of shaping parameters for the λ_j^Ks is given by the formula

$$N_Y = 5(N_{DS1}+1) + 6(N_{DS2}+1). \quad (54)$$

3.2.3. Global optimisation parameters. Additional parameters must be introduced in order to generate a step globally optimised. Global parameters such as the step length, the step time, the step velocity and either sub-phase durations must be adjusted. These variables are not independent. Thus, in the relationship

$$l_{\mathrm{step}} = V_{\mathrm{step}} \times T_{\mathrm{step}}, \quad (55)$$

we consider the mean walking velocity V_{step} over the step under consideration as an input data for the optimisation problem, and the step time T_{step} as a parameter to be optimised. The step length l_{step} is then given by (55).

Moreover, we define the relative durations x_{DS1} and x_{DS2} of double-support sub-phases by setting

$$\begin{aligned} T_{DS1} &= x_{DS1} \times T_{\mathrm{step}}, \\ T_{DS2} &= x_{DS2} \times T_{\mathrm{step}}. \end{aligned}$$

They will be dealt with as further optimisation parameters. The single support time is then defined as

$$T_{\mathrm{SSP}} = (1 - x_{DS1} - x_{DS2}) T_{\mathrm{step}}.$$

In this way, we account for three new optimisation variables we put together in the vector

$$Z = (z_1, z_2, z_3)^T := (T_{\mathrm{step}}, x_{DS1}, x_{DS2})^T. \quad (56)$$

As a final point, optimisation parameters ordered in (49), (53) and (56) may be assembled in the global optimisation vector X^*such that

$$X^* = (X^T, Y^T, Z^T)^T. \quad (57)$$

Accounting for Eqs. (51), (54) and (56), the number N^* of its components is

$$N^* = n_q(N+5) + 5(N_{DS1}+1) + 6(N_{DS2}+1) + 3. \quad (58)$$

3.2.4. Converting the optimisation criterion. The integral criterion (41) must be converted into a function depending on the only components of X^*. First, through Eq. (56),

https://doi.org/10.1017/S0263574709990257 Published online by Cambridge University Press

integration bounds can be expressed as functions of the vector Z as follows:

$$\begin{cases} t_1^*(Z) = t^i + (1 - z_2 - z_3)z_1 \\ t_2^*(Z) = t^i + (1 - z_3)z_1 \\ t_3^*(Z) = t^i + z_1 \end{cases}.$$

Next, through Eqs. (50), (52) and (53), the functions T_i in Eq. (41) can be converted into functions T_i^* such that

$$\begin{cases} t \in I^{\mathrm{SSP}}, T_i^*(X,t) = T_i(\phi(X,t), \dfrac{\partial\phi}{\partial t}(X,t), \dfrac{\partial^2\phi}{\partial t^2}(X,t)) \\ k = 1,2; t \in I^{DSk}, T_i^*(X, Y^{DSk}, t) = T_i(\phi(X,t), \\ \quad \dfrac{\partial\phi}{\partial t}(X,t), \dfrac{\partial^2\phi}{\partial t^2}(X,t), \psi^{DSk}(Y^{DSk}, t)) \end{cases}.$$

The criterion (41) is then approximated by the following function F of X, Y and Z

$$C_\tau \approx F(X,Y,Z) = \frac{1}{z_1 V_{\mathrm{step}}} \sum_{i=1}^{13} \xi_i \times \left(\int_{t^i}^{t_1^*(Z)} T_i^*(X,t)^2 \,\mathrm{d}t + \sum_{k=1,2} \int_{t_k^*(Z)}^{t_{k+1}^*(Z)} T_i^*(X,Y,t)^2 \,\mathrm{d}t \right). \quad (59)$$

Consequently, minimising the criterion C_τ turns into

$$\underset{(X,Y,Z)\in D\subset\Re^{N^*}}{Min} F(X,Y,Z) \quad (60)$$

where D is a feasible set defined by the constraints once they are expressed as functions of X,Y and Z. This transformation is done in the next section.

3.2.5. Converting the constraints. The running time t must be removed from the time-dependent constraints in order to get functions depending on the discrete optimisation variables X, Y and Z only.

First, let us consider equality constraints (4) and (5) as well as the constraint g_{13}^{DS1} in (33). Through the representations (50), (52) and (53), they can be converted into functions of X, Y and t that we assemble into a functions Ψ^K such that

$$K \in \{DS1, DS2\}, t \in I^K, \Psi^K(X,Y,t) = 0 \quad (\in \Re^6). \quad (61)$$

In the same way, inequality constraints (24), (25), (31)–(34) and (36)–(39) may be brought together into functions H^{SSP} and H^K of X and Y satisfying

$$\begin{cases} t \in I^{\mathrm{SSP}}, H^{\mathrm{SSP}}(X,t) \le 0 \quad (\in \Re^{N_{H^{\mathrm{SSP}}}}) \\ K \in \{DS1, DS2\}, t \in I^K, H^K(X,Y,t) \le 0 \quad (\in \Re^{N_{H^K}}) \end{cases}. \quad (62)$$

We have used both following methods to eliminate the running time from the constraints (61) and (62).

3.2.5.1. Discretisation of constraints. This approach consists of satisfying the constraints at a finite number of given instants. Connecting knots of spline functions are logically these control points. Thus, constraints (61) and (62) are taken into account at times t_j^K (Fig. 8) as follows:

$$\begin{cases} 1 \le j \le N_{\mathrm{SSP}} + 1, H^{\mathrm{SSP}}(X, t_j^{\mathrm{SSP}}) < 0 \\ k = 1,2; 1 \le j \le N_{DSk} + 1, \begin{cases} \Psi^{DSk}(X,Y,t_j^{DSk}) = 0. \\ H^{DSk}(X,Y,t_j^{DSk}) < 0 \end{cases} \end{cases} \quad (63)$$

These discrete constraints define the feasible set D of optimisation variables over which the cost function F in Eq. (60) must be minimised. This processing mode for continuous constraints was used to carry out the synthesis of sagittal gait for a 7-link biped.[42,43]

In that way, the initial dynamic optimisation problem is converted into a constrained non-linear optimisation problem with a finite number of discrete variables. The latter can be solved using customised computation codes implementing SQP (Sequential Quadratic Programming) algorithms. These have the ability to fulfil the constraints (63) very accurately.[43,44] However, the original continuous constraints (61) and (62) may oscillate between knots and, consequently, to be infringed. Increasing the number of knots could decrease constraint infringements. Nevertheless, this option results in a greater number of constraints to be dealt with, which might affect the numerical robustness of the computation code employed. Penalty techniques are a means to avoid this problem.

3.2.5.2. Penalty method. We consider the so-called exterior penalty method which consists of minimising the global infringement of constraints. The local infringement can be defined from Eq. (62) as the positive functions

$$\begin{cases} 1 \le i \le N_{H^{\mathrm{SSP}}}, H_i^{\mathrm{SSP}+}(X,t) := \underset{t\in I^{\mathrm{SSP}}}{Max}(0, H_i^{\mathrm{SSP}}(X,t)), \\ k = 1,2; 1 \le i \le N_{H^{DSk}}, \\ \quad H_i^{DSk+}(X,Y,t) := \underset{t\in I^{DSk}}{Max}(0, H_i^{DSk}(X,Y,t)). \end{cases}$$

Then, setting

$$K \in \{\mathrm{SSP}, DS1, DS2\}, H^{K+} = (H_1^{K+}, \ldots, H_{N_{H^K}}^{K+})^T,$$

these functions can be minimised by introducing their quadratic values into an augmented criterion. Equality constraints (61) may be dealt with in the same way. Thus, we consider the penalised cost function:

$$F_p(X,Y,Z) = F(X,Y,Z) + p_i \times \left\{ \int_{t^i}^{t_1^*(Z)} [H^{\mathrm{SSP}+}(X,t)]^T H^{\mathrm{SSP}+}(X,t)\,\mathrm{d}t + \sum_{k=1,2} \int_{t_k^*(Z)}^{t_{k+1}^*(Z)} [H^{DSk+}(X,Y,t)]^T H^{DSk+}(X,Y,t)\,\mathrm{d}t \right\} + p_e \sum_{k=1,2} \int_{t_k^*(Z)}^{t_{k+1}^*(Z)} [\Psi^{DSk+}(X,Y,t)]^T \Psi^{DSk+}(X,Y,t)\,\mathrm{d}t, \quad (64)$$

https://doi.org/10.1017/S0263574709990257 Published online by Cambridge University Press

where p_i and p_e are penalty factors related to inequality and equality constraints respectively. The function F_p must be minimised for given sufficiently great values of p_i and p_e (one can say about 1000) in order to get tiny residual values of the penalty functions, that is to say the quadratic values of constraint infringements.

4. Gait Simulations

The mechanical characteristics of the biped BIP shown in Fig. 1 were used as basic data to carry out the numerical simulations. The geometrical dimensions of the biped and its inertia data are given in Tables A1 and A2 respectively. The forefoot mass is considered as lumped along the toe-joint axis. Therefore, its mass is transferred to the foot inertia.

A 'C' computing code was developed using the Scilab software[57] for programming the parametric optimisation problem formulated in the above section. More specifically, the minimisation problem (60), (63), and its penalised version (64) were solved using the specific code FSQP[58] which implements a Sequential Quadratic Programming algorithm.

As indicated by the flow chart in Fig. 9, a guess solution is required in order for an iterative optimisation process to be initialised. This prerequisite data is taken from a movement constructed in a quite simple way. First, four postural configurations $q(t^i)$, $q(t_1^*)$, $q(t_2^*)$ and $q(t^f)$ of the biped are intuitively defined at end and transition times. The corresponding vectors of generalised velocities $\dot{q}(t^i)$, $\dot{q}(t_1^*)$, $\dot{q}(t_2^*)$ and $\dot{q}(t^f)$ are deduced from a given translatory

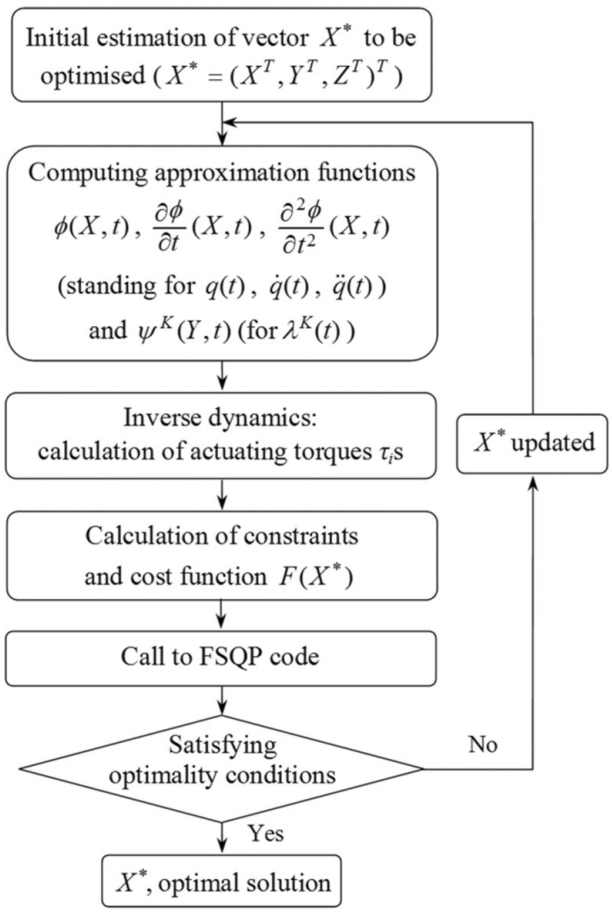

Fig. 9. Algorithmic organisation of the solving iterative process.

velocity for the trunk together with rotation velocities of the feet at t^i, t_1^*, t_2^* and t^f. Thus, each q_i and its derivative $\dot{q}_i$ are determined on each sub-phase by their end values. Then, over every subinterval $[t^i, t_1^*]$, $[t_1^*, t_2^*]$ and $[t_2^*, t^f]$, the q_is may be interpolated by cubic time-functions. This representation was used to provide estimated values q_{ik}s for the q_is at control knots t_k^K (see Fig. 8 for notations). In this manner, we obtained a set of values defining the vector X of Eq. (48) through the sequence of vectors X^is in Eq. (47).

In a similar way, an initialising value for the vector Y (Section 3.2.2) is required. As this one represents the contact forces acting on the front foot, we simply defined its values at end times t_1^*, t_2^* and t^f of the double support sub-phases by allocating an increasing fraction of the biped weight as normal contact forces at successive end times. Linear interpolations computed between these end values at knots t_k^K (for $K \in \{DS1, DS2\}$) provide the expected initialising components of vector Y.

The vector Z (Section 3.2.3) is made up of three parameters representing the step time and the relative durations of sub-phases $DS1$ and $DS2$. Both sub-phase times could be chosen between 10 and 20 per cent of the total step time.

The initialising vector X^* resulting from the above vectors X, Y and Z is accepted as an initial solution by the optimisation routine FSQP. Consequently, there is no need to optimise partly each sub-phase prior to a global optimisation as it was done previously for sagittal gait synthesis.[42–44] The step cycle can be directly and globally optimised.

Two simulations of purely cyclic steps are presented. In both cases, the time cycle was divided into 10 subintervals, four for the single support and three for each sub-phase of the double support. The formula (58) defined for $n_q = 13$, $N = 10$, and $N_{DS1} = N_{DS2} = 3$, yields a number of 242 optimisation parameters.

The step width is equal to 0.18 m for the two simulations. The walking velocities are equal to 0.75 ms^{-1} and 1.25 ms^{-1} in the first and second simulation respectively.

4.1. Simulation 1

The Fig. 10 gives an insight in 3D-isometric perspective of the gait pattern generated. In Fig. 11, the same movement is projected on the horizontal and frontal planes of the reference frame $(O; X_0, Y_0, Z_0)$. The first projection shows that the swing leg slightly moves away from the sagittal plane. The second reveals a moderate transversal movement of the pelvis-trunk. The sagittal projection in Fig. 12 shows that both legs are noticeably flexed at step ends. Conversely, the stance leg is moderately extended at mid-swing with a correlative lift up of the trunk, and the swing leg is almost fully extended near the end of single support. The need for pronounced leg flexions and extensions is most likely required to compensate for the absence of heel lift-off phase of the stance foot before the end of single support.

In Fig. 13, one can observe that the horizontal components of contact forces under both feet have quite moderate values in comparison with their normal counterpart. The dry friction coefficient could be smaller than 0.3.

Actuating torques of the stance leg (Fig. 14) have obviously bigger values than their swing leg counterparts (Fig. 15). The

https://doi.org/10.1017/S0263574709990257 Published online by Cambridge University Press

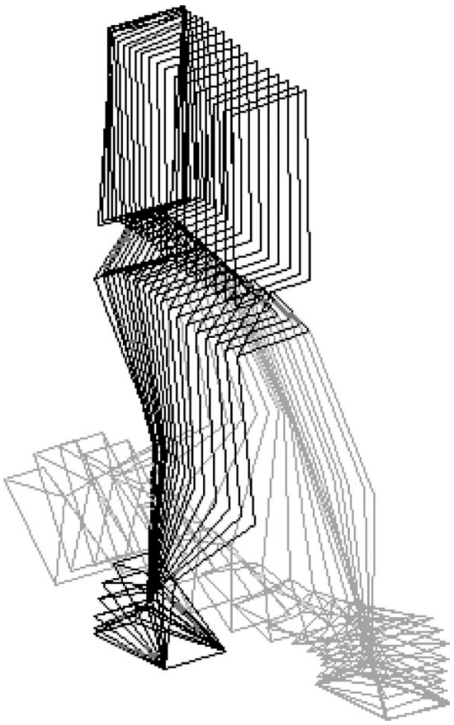

Fig. 10. 3D-isometric view of the optimised step-sequence SSP–DSP.

propulsive effect is essentially due to torques $T3$, $T4$ and $T5$ which power the flexion-extension movements at ankle, knee and hip during the three step sub-phases. Especially, torques $T3$ and $T5$ at ankle and hip exhibit finite quasi impulsive values at beginning of the sub-phase $DS1$. It should be noticed that the hip adduction-abduction torque $T7$ takes significant

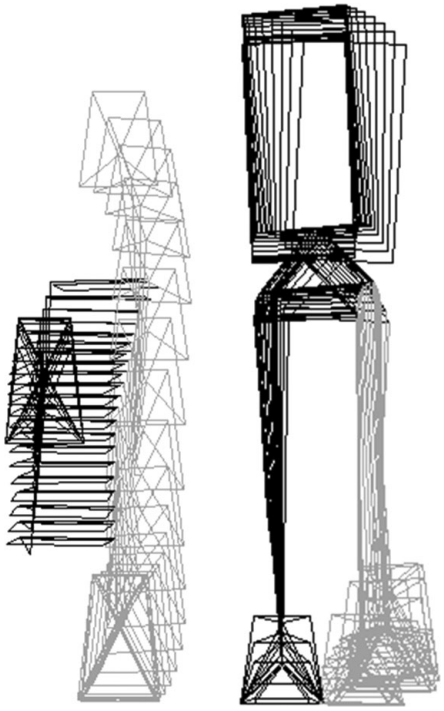

Fig. 11. Horizontal and frontal projections of the step movement.

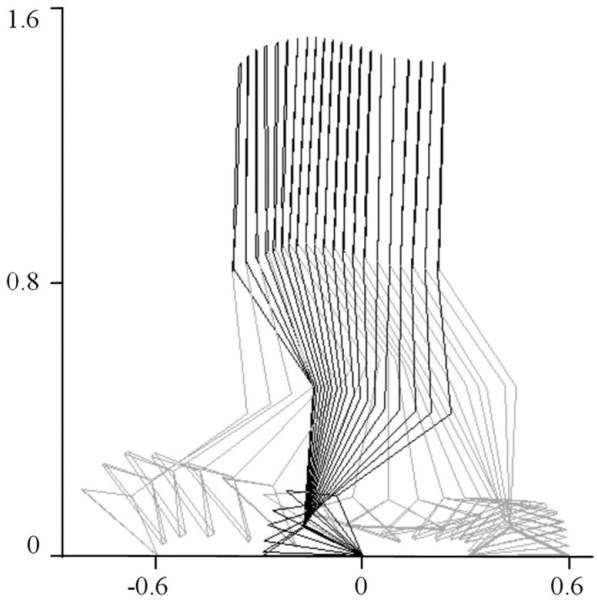

Fig. 12. Sagittal projection of the step movement.

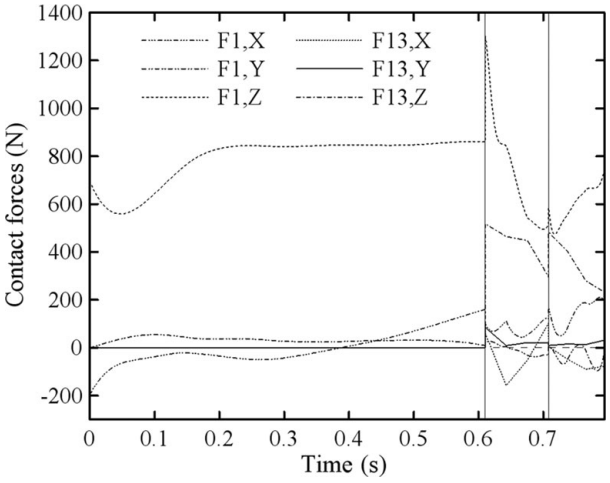

Fig. 13. Evolution of components of the contact force under each foot during the three successive sub-phases SSP, $DS1$ and $DS2$ which are separated by vertical full lines.

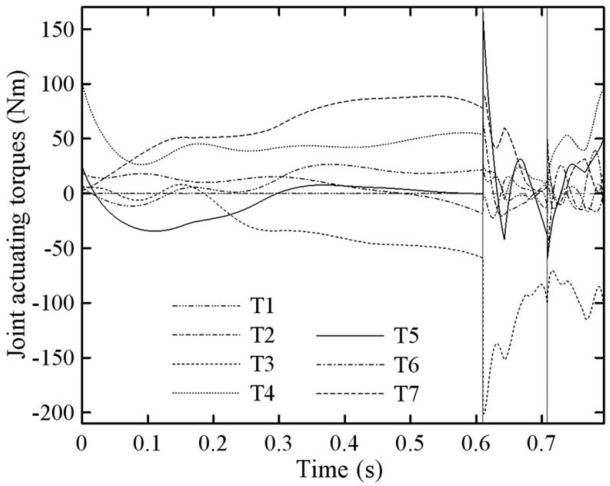

Fig. 14. Evolution of joint actuating torques of the stance leg.

https://doi.org/10.1017/S0263574709990257 Published online by Cambridge University Press

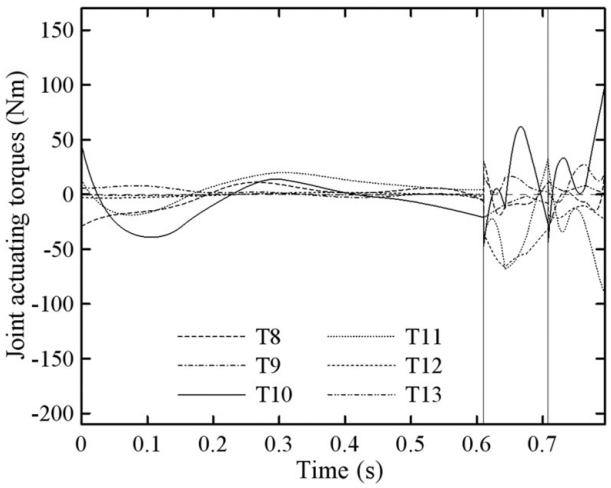

Fig. 15. Evolution of joint actuating torques of the swing leg.

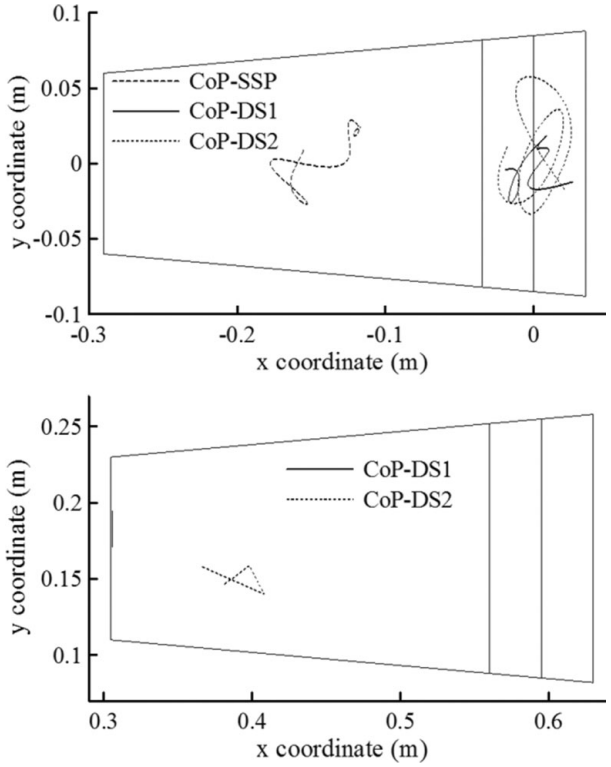

Fig. 16. CoP trajectories on each footprint, under the foot and fore-foot (stance foot at the top of figure).

values during the single support, due to the fact that the trunk is overhanging on the stance leg hip in the frontal plane.

In Fig. 16, the *CoP* trajectories of the stance foot show that the contact with the ground remains well balanced during the single support as well as during the double support through which the contact is limited to the fore-foot. The *CoP* of the front foot (at bottom of the figure) is first closely located on the heel edge during the *DS*1 sub-phase, then, through the *DS*2 sub-phase, it describes a closely located broken line of which nature is due to the fact that the contact forces under the front foot were approximated by piecewise linear functions.

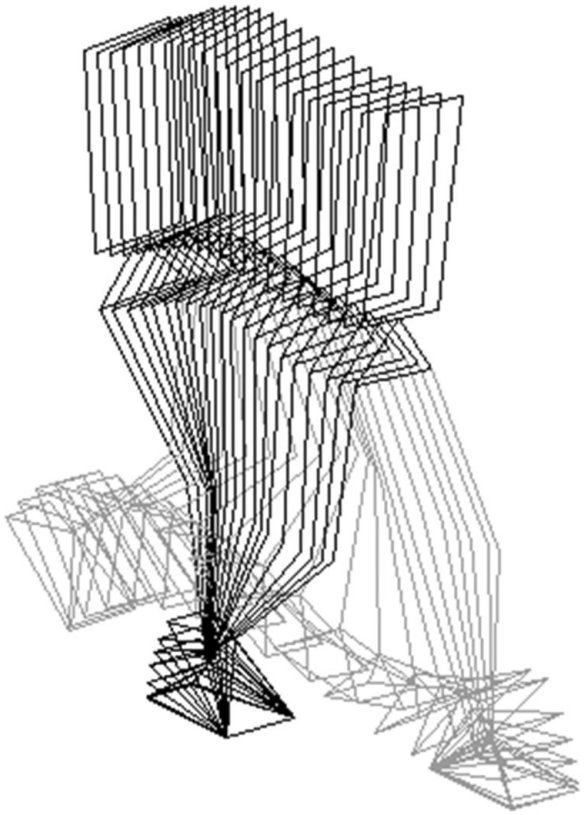

Fig. 17. 3D-isometric view of the optimised step sequence SSP-DSP.

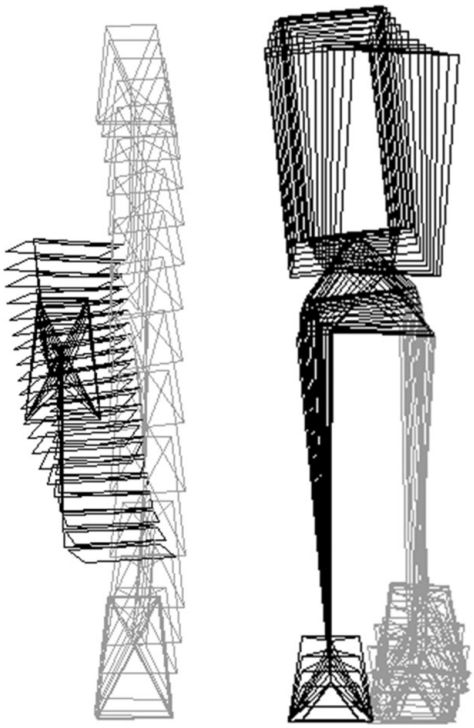

Fig. 18. Horizontal and frontal projections of the step movement.

4.2. Simulation 2

The only difference with respect to the previous example is the walking velocity which is equal here to 1.25 ms^{-1} (instead of 0.75 ms^{-1}).

Successive Figs. 17–19 reveal clearly the step lengthening when compared with the previous Figs. 10–12. One can

https://doi.org/10.1017/S0263574709990257 Published online by Cambridge University Press

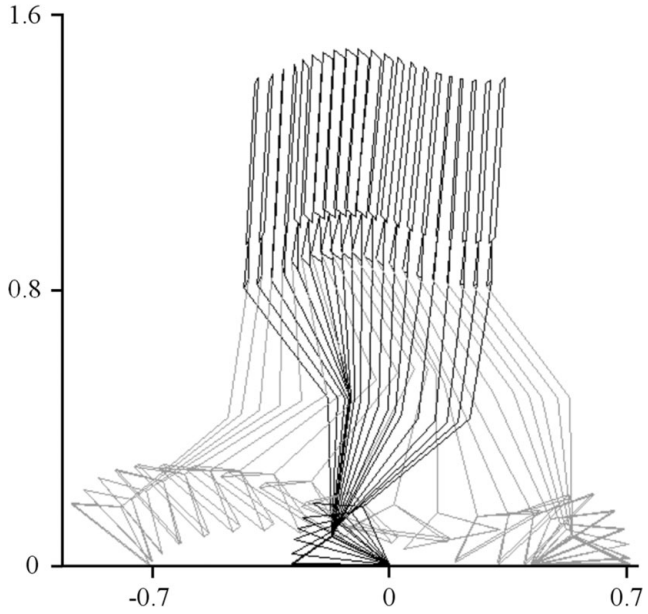

Fig. 19. Sagittal projection of the step movement.

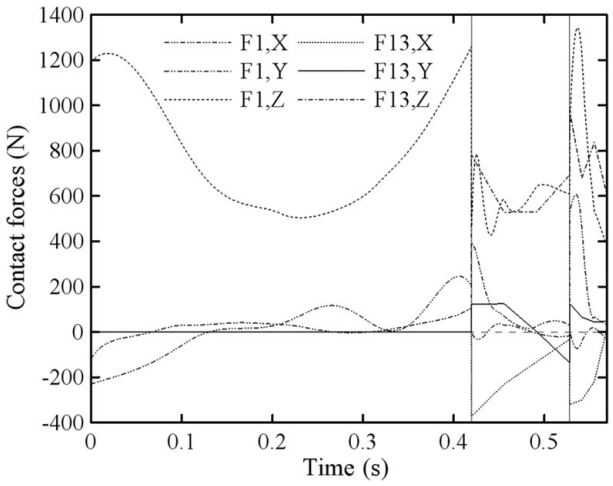

Fig. 20. Evolution of components of the contact force under each foot.

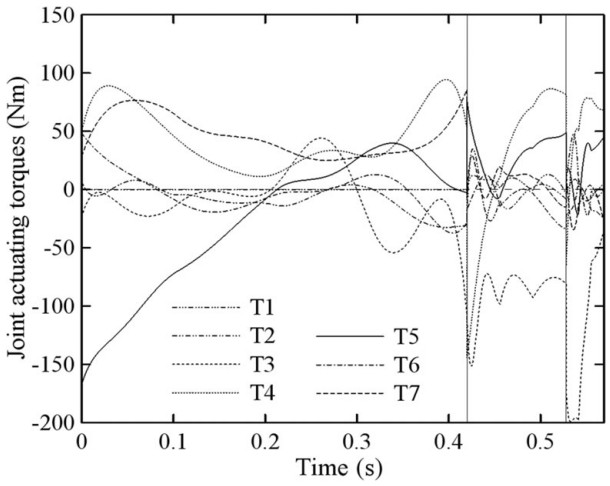

Fig. 21. Evolution of joint actuating torques of the stance leg.

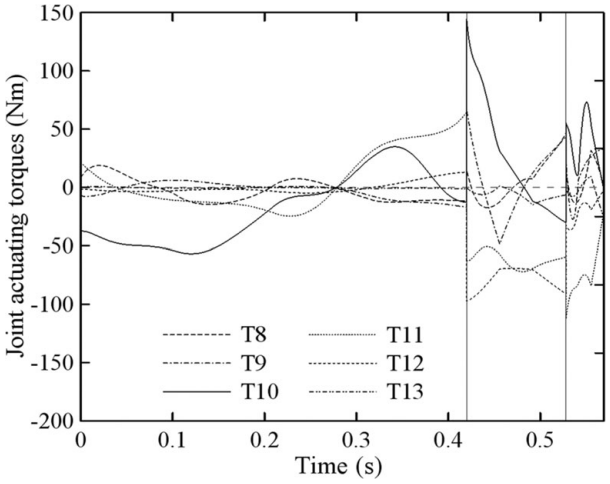

Fig. 22. Evolution of joint actuating torques of the swing leg.

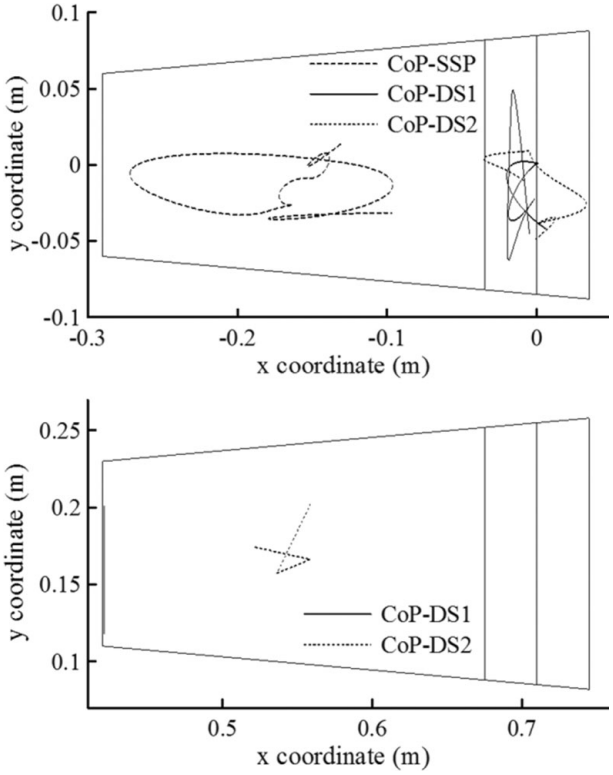

Fig. 23. CoP trajectories on each footprint, under the foot and fore-foot.

notice that the swing leg does not deviate significantly from the sagittal plane (Fig. 18). On the other hand, the transversal movement of the trunk has a bigger magnitude than its preceding counterpart. Figure 19 shows that the trunk has a transversal rotation as observed in human gait.[59]

Contact forces (Fig. 20) and actuating torques (Figs. 21 and 22) take greater extremal values than their former counterparts. Non-sliding on the stance foot during the *DS*2 sub-phase requires a dry friction coefficient not smaller than 0.45. Actuating torques have more variations than those of the previous case, but with extremal values that do not exceed the limit of 200 Nm.

The trajectories of the centres of pressure on the footprints are quite similar to the curves observed in the first simulation.

https://doi.org/10.1017/S0263574709990257 Published online by Cambridge University Press

Table I. Summary of results.

Forward velocity (ms^{-1})	0.75	1.25
Step length L_{step} (m)	0.595	0.712
Step time T_{step} (s)	0.79	0.57
Sub-phase $DS1$ (% T_{step})	12.4	18.7
Sub-phase $DS2$ (% T_{step})	10.8	7.3
Energy expended per metre (Jm^{-1})	324	432

However, the circulation areas of the CoPs are larger than in the first case. This situation is related to the fact that frontal, transversal and lateral movements of the biped have greater amplitudes than their corresponding movements in the first simulation.

The results summarised in Table I, first show the increase of the step length (about 20%) versus the walking velocity. Next, the relative times of sub-phases $DS1$ and $DS2$ show that the double support duration amounts to 23.2% of the time cycle for the lowest velocity and 26% for the other. This result is consistent with earlier results obtained for sagittal gait.[44] Finally, the energy spent per unit of distance travelled is shown in the last line.

Both numerical examples demonstrate the effectiveness of the method used for generating compound movements of high-degrees-of-freedom multibody systems as humanoid robots. The results could be enhanced by using a greater number of interpolating subintervals and by improving or modifying the level of constraint satisfaction. The movements generated may help to gain deeper insight into gait dynamics. They could be implemented as reference movements to be tracked using an appropriate robot controller.

5. Concluding Remarks

A method for achieving dynamic synthesis of walking steps was developed using an optimisation approach. A parametric optimisation technique was used to cope with the complexity of the stated dynamic optimisation problem. The numerical process performs as a walking pattern generator based on the minimisation of actuating torques. This criterion is the basic organising principle of the movement. The latter is also generated on the base of a limited set of characteristic constraints excluding any given data defined along the motion time. The data required for generating a purely cyclic step can be reduced to the walk speed. The numerical process has the ability to generate the whole movement including particularly the step length, the length of each sub-phase, and the postural states of transition and end configurations of the step. A prominent problem dealt with for achieving dynamic synthesis of gait was related to ground-foot contact handling. First, in accordance with the contact pattern taken into consideration, appropriate locations of footholds were obtained by constraining efficiently both centres of pressure on their respective footprints. This is to ensure the control of the biped balance on its ground supports. Next, undetermined dynamics arising through the double support must be treated so as to avoid useless stress in the locomotion system and to clear up the biped overactuation. This was done by means of an optimal adjustment of contact forces achieved through the parameterisation of the wrench exerted by the ground on the front foot.

A variety of additional simulations could be directly carried out such as, for example, generating start and stop steps, accelerated and decelerated steps, turning steps and walking up and down stairs. Even more simply, the inertia model may be changed. The mass distribution of the biped BIP has disproportionate values for the trunk in comparison with the inertia models of more recent humanoids. Further simulations might be carried out for generating gait patterns for such walking robots. The biometric model of a human walker could be employed as well to achieve human gait synthesis. In this respect, it should be noticed that the dynamic model used for the simulations shown in this paper is qualitatively closer to a human model than a humanoid model as it does not account for joint friction. Dry friction can affect significantly the dynamic behaviour of a multibody system. Appropriate friction laws could easily be introduced in the dynamic model. As the optimisation method is based on the use of a finite number of discrete optimisation parameters, the presence of discontinuities induced by dry friction does not change the algebraic nature of the problem to be solved.

Furthermore, it should be interesting to extend the dynamic model to supplementary degrees of freedom by considering arms and a pelvis-trunk joint in order to simulate more accurately human gait and humanoid walking. The number of useful further degrees of freedom could be three for a pelvis-trunk spherical linkage plus one flexion-extension rotation at shoulder for each arm. Accounting for 18 degrees of freedom instead of 13 as above should not increase considerably the order of computational complexity of the resulting optimisation problem, especially due to the fact that such additional degrees of freedom would not introduce new constraining conditions on contact forces which are by far the hardest to be dealt with.

Appendix 1. Denavit–Hartenberg's construction applied to biped BIP

The reader is referred to Khalil–Dombre[51] for a general presentation of this geometrical construction. We apply it to the kinematic structure shown in Fig. 1 which represents the locomotion system of the biped BIP[43,44] (Fig. 24).

First, an axial direction is defined on each joint axis using a unit vector Z_i for the ith joint. The construction is based on the introduction of the common perpendicular to both successive axes $(O_{i-1}; Z_{i-1})$and $(O_i; Z_i)$ for each subscript i (Fig. 1). Using Khalil-Kleinfinger's notations,[51] the unit vector $X_{i-1} = O_{i-1}O'_i / \| O_{i-1}O'_i \|$ is introduced, and the following geometric parameters are defined:

- $d_i = O_{i-1}O_i \cdot X_{i-1}$, $r_i = O_{i-1}O_i \cdot Z_i$
- $\alpha_i = (Z_{i-1}, Z_i)$, angle oriented by X_{i-1}
- $q_i = (X_{i-1}, X_i)$, angle oriented by Z_i

where q_i represents the rotation of link (S_i) with respect to link (S_{i-1}).

For every subscript i, the local frame $Fr_i = (O_i; X_i, Y_i, Z_i)$, $Y_i = Z_i \times X_i$, is attached to the body segment (S_i). The numerical values of the set of geometrical

https://doi.org/10.1017/S0263574709990257 Published online by Cambridge University Press

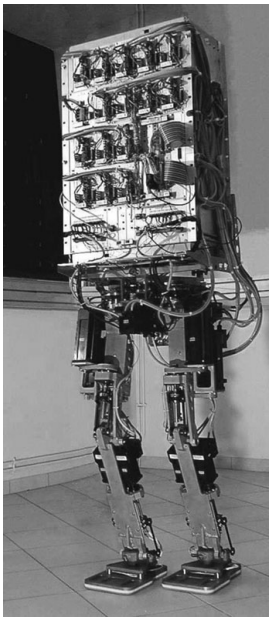

Fig. 24. Biped BIP (LMS, University of Poitiers; INRIA-RA, Grenoble, France).

Table AI. Biped geometrical dimensions and setting of local frames.

Local frames	d_i (m)	r_i (m)	α_i	q_i-*init*
Fr_1	0	0	$-\pi/2$	$-\pi/2$
Fr_2	0.083	−0.17	$-\pi/2$	0
Fr_3	0	0	$\pi/2$	0
Fr_4	0.41	0	0	0
Fr_5	0.41	0	0	$\pi/2$
Fr_6	0	0	$\pi/2$	$\pi/2$
Fr_7	0	0	$\pi/2$	0
Fr_8	0.22	0	0	0
Fr_9	0	0	$-\pi/2$	$-\pi/2$
Fr_{10}	0	0	$-\pi/2$	$\pi/2$
Fr_{11}	0.41	0	0	0
Fr_{12}	0.41	0	0	0
Fr_{13}	0	0	$\pi/2$	0

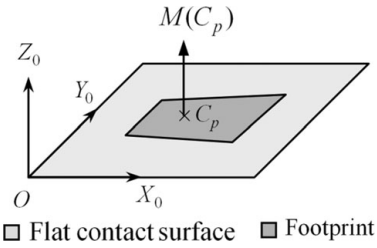

Fig. 25. The moment $M(C_p)$ of contact forces at the centre of pressure C_p is normal to the footprint.

parameters d_i, r_i and α_i described above are given in Table AI. The biped inertia data is given in Table AII.

Appendix 2. Location of the centre of pressure

Knowing that (Fig. 25)

$$M(C_p) \times Z_0 = 0, \tag{A2.1}$$

the location of the centre of pressure is given by the function

$$OC_p = \frac{Z_0 \times M(O)}{Z_0 \cdot R}, \tag{A2.2}$$

where Z_0 is the normal unit vector to the footprint, $M(O)$ is the moment at given point O, and R the resultant of contact forces exerted by the ground.

Proof. $M(O)$ and $M(C_p)$ are correlated by the well-known relationship

$$M(O) = M(C_p) + OC_p \times R.$$

Multiplying by Z_0 and accounting for (A2.1), one gets

$$Z_0 \times M(O) = Z_0 \times (OC_p \times R).$$

Table AII. Inertia data of biped BIP (see Fig. 1).

Body segments	Mass (kg)	Local coordinates in Fr_i of centres of mass G_i (m)			Inertia matrix components of S_i in the local frame $(G_i; X_i, Y_i, Z_i)$(m^2 kg)					
S_i	m_i	a_i	b_i	c_i	A^i_{XX}	B^i_{YY}	C^i_{ZZ}	D^i_{ZX}	E^i_{XY}	F^i_{YZ}
S_1	2.34	0.024	−0.151	0.0	0.07	0.0	0.07	0.0	0.0	0.0
S_2	0.18	0.0	0.0	0.0	0.0	0.0	0.0	0.0	0.0	0.0
S_3	5.93	0.258	−0.028	0.0	0.02	0.47	0.47	0.0	0.0	0.04
S_4	10.9	0.25	−0.005	−0.045	0.06	0.82	0.8	0.0	0.15	0.01
S_5	0.7	−0.002	−0.034	0.0	0.0	0.0	0.0	0.0	0.0	0.0
S_6	3.2	−0.005	0.107	0.029	0.06	0.0	0.05	0.0	0.0	0.0
S_7	58.3	0.11	0.44	0.012	5.86	1.11	6.75	−0.02	0.07	−1.53
S_8	3.2	0.005	0.029	−0.107	0.06	0.05	0.0	0.0	0.0	0.0
S_9	0.7	−0.002	0.0	0.034	0.0	0.0	0.0	0.0	0.0	0.0
S_{10}	10.9	0.16	0.005	0.045	0.06	0.42	0.39	0.0	−0.05	0.0
S_{11}	5.93	0.152	0.028	0.0	0.02	0.21	0.21	0.0	0.0	−0.03
S_{12}	0.18	0.0	0.0	0.0	0.0	0.0	0.0	0.0	0.0	0.0
S_{13}	2.34	0.059	0.0	0.019	0.02	0.03	0.01	0.0	−0.01	0.0

https://doi.org/10.1017/S0263574709990257 Published online by Cambridge University Press

We can extract $OC_p \times R$ as an unknown X in a vector equation of the type $U \times X = V$ of which solution is (provided that $U \neq 0$ and $U \cdot V = 0$)

$$X = -\frac{U \times V}{\|U\|^2} + \lambda U, \quad \lambda \in \Re.$$

Since $\|Z_0\| = 1$, this result yields

$$OC_p \times R = -Z_0 \times (Z_0 \times M(O)) + \lambda Z_0, \quad \lambda \in \Re.$$

Multiplying again by Z_0 gives

$$Z_0 \times (OC_p \times R) = -Z_0 \times (Z_0 \times (Z_0 \times M(O))).$$

Developing each member using the formula $U \times (V \times W) = (U \cdot W)V - (U \cdot V)W$, and knowing that $Z_0 \cdot OC_p = 0$, this equation simply becomes

$$(Z_0 \cdot R)OC_p = Z_0 \times M(O),$$

which provides the expected result (Table AII).

References

1. S. H. Collins, M. Wisse and A. Ruina, "A three-dimensional passive-dynamic walking robot with two legs and knees," *Int. J. Robot. Res.* **20**, 607–615 (2001).
2. S. H. Collins and A. Ruina, "A Bipedal Walking Robot with Efficient and Human-Like Gait," *Proceedings of the IEEE International Conference on Robotics and Automation*, Barcelona, Spain (2005) pp. 1983–1988.
3. S. H. Collins, A. Ruina, M. Wisse and R. Tedrake, "Efficient bipedal robots based on passive-dynamic walkers," *Science* **307**, 1082–1085 (2005).
4. T. McGeer, "Passive dynamic walking," *Int. J. Robot. Res.* **9**, 62–82 (1990).
5. T. McGeer, "Passive Walking with Knees," *Proceedings of IEEE International Conference on Robotics and Automation*, Cincinnati, Ohio (1990) pp. 1640–1645.
6. A. Goswami, B. Espiau and A. Keramane, "Limit cycles in a passive compass gait biped and passivity-mimicking control laws," *J. Auton. Robots* **4**(3), 273–286 (1997).
7. M. Garcia, A. Chatterjee and A. Ruina, "Speed, Efficiency, and Stability of Small-Slope 2-D Passive Dynamic Bipedal Walking," *Proceedings of IEEE International Conference on Robotics and Automation*, Leuven, Belgium (1998) pp. 2351–2356.
8. M. Garcia, A. Ruina and M. Coleman, "Some Results in Passive-Dynamic Walking," *Proceedings of the Euromech Conference on Biology and Technology of Walking*", Prague, Czech Republic (1998) pp. 268–275.
9. J. K. Holm, D. Lee and M. W. Spong, "Time-Scaling Trajectories of Passive-Dynamic Bipedal Robots," *Proceedings of IEEE International Conference on Robotics and Automation*, Roma, Italy (2007) pp. 3603–3608.
10. M. Wisse, Essentials of dynamic walking; analysis and design of two-legged robots *Ph. D. Thesis* (Delf, The Netherlands: Technische Universiteit, 2004).
11. S. H. Collins and A. Ruina, "A Bipedal Walking Robot with Efficient and Human-Like Gait," *Proceedings of IEEE International Conference on Robotics and Automation*, Barcelona, Spain (2005) pp. 1983–1988.
12. F. Leboeuf, G. Bessonnet, P. Seguin and P. Lacouture, "Energetic versus sthenic optimality criteria for gymnastic movement synthesis" *Multibody Syst. Dyn.* **16**, 213–236 (2006).
13. M. Gienger, K. Löffler and F. Pfeiffer, "A Biped Robot that Jogs," *Proceedings of IEEE International Conference on Robotics and Automation*, San Francisco, CA (2000) pp. 3334–3339.
14. M. Hirose, Y. Haikawa, T. Takenaka and K. Hirai, "Development of Honda Humanoid Robot ASIMO," *Proceedings of IEEE/RSJ International Conference on Intelligent Robotic and Systems* (Seoul, South Korea, 2001).
15. K. Yokoi, F. Kanehiro, K. Kaneko, S. Kajita, K. Fujiwara and H. Hirukawa, "Experimental Study of Humanoid Robot HRP-1S," *Int. J. Robot. Res.* **23**, 351–362 (2004).
16. Y. Ogura, H. Aikawa, K. Shimomura, H. Kondo, A. Morishima, H. Lim and A. Takanishi, "Development of a New Humanoid Robot WABIAN-2," *Proceedings of IEEE International Conference on Robotics and Automation*, Orlando, Florida (2006) pp. 76–81.
17. K. Akashi, K. Kaneko, N. Kanehira, S. Ota, G. Miyamori, M. Hirata, S. Kajita and K. Kanehiro, "Development of Humanoid Robot HRP-3P" *Proceedings of the IEEE-RAS International Conference on Humanoid Robots*, Tsukuba, Japan (2005) pp. 50–55.
18. M. Vukobratovic and J. Stepanenko, "On the stability of anthropomorphic systems," *Math. Biosci.* **15**(1), 1–37 (1972).
19. M. Vukobratovic, B. Borovac, D. Surla and D. Stokic, *Biped Locomotion: Dynamics, Stability, Control and Applications* (Springer-Verlag, Berlin, 1990).
20. M. Vukobratovic and B. Borovac, "Zero-moment point – Thirty five years of its life," *Int. J. Human. Robot.* **1**(1), 157–173 (2004).
21. K. Hirai, M. Hirose, Y. Haikawa and T. Takenaka, "The Development of Honda Humanoid Robot," *Proceedings of IEEE International Conference on Robotics and Automation*, Leuven, Belgium (1998) pp. 160–165.
22. K. Mitobe, G. Capi and Y. Nasu, "Control of walking robots based on manipulation of the zero moment point," *Robotica* **18**, 651–657 (2000).
23. Q. Huang, K. Yokoi, S. Kajita, K. Kaneko, H. Arai, N. Koyachi and K. Tanie, "Planning walking patterns for a biped robot," *IEEE Trans. Robot. Autom.* **17**(3), 280–289 (2001).
24. F. Pfeiffer, K. Löffler and M. Gienger, "Humanoid robots," *Proceedings of the 6th International Conference on Climbing and Walking Robots* (2003) pp. 505–516.
25. K. Löffler, M. Gienger and F. Pfeiffer, "Sensors and control concept of walking «Johnnie»," *Int. J. Robot. Res.* **22**(3–4), 229–239 (2003).
26. F. Kanehiro, H. Hirukawa and S. Kajita, "Open HRP: Open architecture humanoid robotics platform," *Int. J. Robot. Res.* **23**(2), 155–165 (2004).
27. J.-E. Pratt and G.-A. Pratt, "Exploiting Natural Dynamics in the Control of a 3D Bipedal Walking Simulation," *Proceedings of International Conference on Climbing and Walking Robots*, Portsmouth, UK (1999) pp. 797–807.
28. S. Kajita, O. Matsumoto and M. Saigo, "Real-Time 3D Walking Pattern Generation for a Biped Robot with Telescopic Legs," *Proceedings of IEEE International Conference on Robotics and Automation* (2001) pp. 2299–2306.
29. C.-M. Chew and G.-A. Pratt, "Frontal Plane Algorithms for Dynamic Bipedal Walking," *Proceedings of IEEE International Conference on Robotics and Automation*, Taipei, Taiwan (2003) pp. 45–50.
30. H. Hirukawa, F. Kanehiro, S. Kajita, K. Fujiwara, K. Yokoi, K. Kaneko and K. Harada, "Experimental Evaluation of the Dynamics Simulation of Biped Walking of Humanoid Robots," *Proceedings of IEEE International Conference on Robotics and Automation*, Taipei, Taiwan (2003) pp. 1640–1645.
31. K. Löffler, M. Gienger and F. Pfeiffer, "Sensors and control concept of walking «Johnnie»," *Int. J. Robot. Res.* **22**(3–4), 229–239 (2003).
32. A. Takanishi, H. Lim, M. Tsuda and I. Kato, "Realization of Biped Dynamic Walking Stabilized by Trunk Motion on a Sagittally Uneven Surface," *Proceedings of IEEE International*

https://doi.org/10.1017/S0263574709990257 Published online by Cambridge University Press

Workshop on Intelligent Robots and Systems, *IROS'90*, Ibaraki, Japan (1990) pp. 323–330.
33. Q. Li, A. Takanishi and I. Kato, "Learning Control for a Biped Walking Robot with a Trunk," *Proceedings IEEE/RSJ International Conference on Intelligent Robots and Systems*, Yokohama, Japan (1993) pp. 1771–1777.
34. C. K. Chow and D. H. Jacobson, "Studies of human locomotion via optimal programming," *Math. Biosci.* **10**, 239–306 (1971).
35. G. Bessonnet, S. Chessé and P. Sardain, "Optimal motion synthesis – Dynamic modelling and numerical solving aspects," *Multibody Syst. Dyn.* **8**, 257–278 (2002).
36. G. Bessonnet, S. Chessé and P. Sardain, "Optimal gait synthesis of a seven-Link planar biped," *Int. J. Robot. Res.* **33**, 1059–1073 (2004).
37. G. Bessonnet and S. Chessé, "Optimal dynamics of actuated kinematic chains – Part 2: Problem statements and computational aspects," *Eur. J. Mech. A/Solids* **24**, 472–490 (2005).
38. V. V. Beletskii and P. S. Chudinov, "Parametric optimisation in the problem of biped locomotion," *Mech. Solids* **12**(1), 25–35 (1977).
39. P. H. Channon, S. H. Hopkins and D. T. Pham, "Derivation of optimal walking motions for bipedal walking robot," *Robotica* **10**, 165–172 (1992).
40. C. Chevallereau and Y. Aoustin, "Optimal reference trajectories for walking and running of a biped robot," *Robotica* **19**, 557–569 (2001).
41. A. Muraro, C. Chevallereau and Y. Aoustin, "Optimal trajectories for a quadruped robot with *trot*, *amble* and *curvet* gaits for two energetic criteria," *Multibody Syst. Dyn.* **9**, 39–62 (2003).
42. T. Saidouni and G. Bessonnet, "Generating globally optimised sagittal gait cycles of a biped robot," *Robotica* **21**, 199–210 (2003).
43. P. Seguin and G. Bessonnet, "Generating optimal walking cycles using spline-based state-parameterization," *Int. J. Human. Robot.* **2**, 47–80 (2005).
44. G. Bessonnet, P. Seguin and P. Sardain, "A parametric optimization approach to walking pattern synthesis," *Int. J. Robot. Res.* **24**, 523–536 (2005).
45. J. Denk and G. Schmidt, "Synthesis of Walking Primitive Databases for Bipeds in 3D-Environments," *Proceedings of IEEE International Conference on Robotics and Automation*, Taipei, Taiwan (2003) pp. 1343–1349.
46. F. Plestan, J. W. Grizzle, E. R. Vestervelt and G. Abba, "Stable walking of a 7-DOF biped robot," *IEEE Trans. Robot. Autom.* **19**(4), 653–668 (2003).
47. D. Djoudi, C. Chevallereau and J. W. Grizzle, "A Path-Following Approach to Stable Bipedal Walking and Zero Moment Point Regulation," *Proceedings of IEEE International Conference on Robotics and Automation*, Roma, Italy (2007) pp. 3597–3602.
48. H. Hirukawa, F. Kanehiro, S. Kajita, K. Fujiwara, K. Yokoi, K. Kaneko and K. Harada, "Experimental Evaluation of the Dynamics Simulation of Biped Walking of Humanoid Robots," *Proceedings of IEEE International Conference on Robotics and Automation*, Taipei, Taiwan (2003) pp. 1640–1645.
49. S. Kajita, K. Kaneko, M. Morisawa, S. Nakaoka and H. Hirukawa, "ZMP-Based Biped Running Enhanced by Toe Springs," *Proceedings of IEEE International Conference on Robotics and Automation*, Taipei, Taiwan (2003) pp. 3963–3969.
50. J. Marot, Contribution à la synthèse dynamique optimale de la marche *PhD Thesis* (Poitiers, France: University of Poitiers, 2007) (in French).
51. W. Khalil and E. Dombre, *Modelling, Identification and Control of Robots* (Butterworth Heinemann, Oxford, UK, 2004).
52. W. Blajer and W. Schiehlen, "Walking without impacts as a motion/force control problem," *ASME J. Dyn. Syst. Meas. Control* **114**, 660–665 (1992).
53. C. Chevallereau, G. Bessonnet, G. Abba and Y. Aoustin, "Les robots marcheurs bipèdes – modélisation, conception, synthèse de la marche, commande," *Hermès*, Paris (2007).
54. S. Miossec and Y. Aoustin, "A Simplified Stability Study for a Biped Walk with Underactuared and Overactuated Phases," *Int. J. Robot. Res.* **24**(7), 537–551 (2005).
55. D. G. Hull, "Conversion of Optimal Control Problems into Parameter Optimization Problems," *J. Guid. Control Dyn.* **20**, 57–60 (1997).
56. J. T. Betts, "Practical methods for optimal control using nonlinear programming," *SIAM* (2001).
57. Scilab-4.0, Consortium Scilab (INRIA, ENPC, Copyright© 1989–2006 (2006).
58. C. T. Lawrence, J. L. Zhou and A. L. Titts, "User's Guide for CFSQP Version 2.3: A C Code for Solving (Large Scale) Constrained Nonlinear (Minimax) Optimization Problems, Generating Iterates Satisfying all Inequality Constrained," *Institute for Systems Research* (College Park, Maryland, 1995).
59. J. Rose and G. J. Gamble, *Human Walking*, 2nd ed. (William & Wilkins, Baltimore, 1994).